

New Ionophoric Calix[4]diquinones: Coordination Chemistry, Electrochemistry, and X-ray Crystal Structures

Paul D. Beer,^{*,†} Philip A. Gale,^{*,†} Zheng Chen,^{†,‡} Michael G. B. Drew,[§] Jennifer A. Heath,[†] Mark I. Ogden,^{†,||} and Harold R. Powell[⊥]

Inorganic Chemistry Laboratory, University of Oxford, South Parks Road, Oxford OX1 3QR, U.K., Department of Chemistry, University of Reading, Whiteknights, Reading RG6 6AD, U.K., and Cambridge Crystallographic Data Centre, 12 Union Road, Cambridge CB1 2EZ, U.K.

Received April 25, 1997[Ⓢ]

A new library of ionophoric *p*-tert-butylcalix[4]diquinones containing ester (**1**), primary, secondary, and tertiary amide (**2–4**), and crown ether (**5**) substituents has been synthesized by treatment of the respective 1,3-bis-substituted *p*-tert-butylcalix[4]arene with Ti(OCOCF₃)₃ in trifluoroacetic acid. The structures of the free ligands **1** and **2**, a *p*-tert-butylcalix[4]diquinone bridged at the lower rim by two linked veratrole groups (**7**), and a previously synthesized *p*-tert-butylcalix[4]diquinone bis(methyl ether) species (**8**) have been elucidated by X-ray crystallography. The X-ray crystal structures of 1-Sr(ClO₄)₂, 1-KClO₄, 2-NaClO₄, 4-*n*-BuNH₃BF₄, 5-NaOCOCF₃, and 5-KPF₆ demonstrate that these complexes adopt the cone conformation in the solid state. Interestingly, cation–quinone oxygen atom coordination occurs at both the upper and lower rim of 2-NaClO₄ and 4-*n*-BuNH₃BF₄. Solution coordination properties have been studied by both ¹H NMR and UV/vis techniques. The electrochemical properties of the “acyclic” *p*-tert-butylcalixdiquinones **1**, **4**, and **8** and their complexes have been studied using cyclic and square wave voltammetric techniques. The reduction potentials of the group 1 or 2 metal, ammonium, and alkylammonium complexes are significantly anodically shifted with respect to that of the free ligand. Addition of cations to electrochemical solutions of a *p*-tert-butylcalixdiquinone–crown-5 compound (**5**) caused large anodic shifts (by up to 555 mV in the presence of Ba²⁺) in a manner similar to that of the acyclic species.

Introduction

With the aim of advancing chemical sensor technology, considerable recent attention has focused on a new generation of abiotic host molecules that contain signaling or responsive functional groups as an integral part of a host macrocyclic framework.¹ The incorporation of a redox-active and/or optical signaling group coupled to a guest binding site enables the host to be used as a sensor for target guest species. The presence of a particular guest may then be detected as a perturbation in the electrochemical and/or photophysical properties of the host. A number of research groups,² including our own,^{1b–d,3} have incorporated redox-active transition-metal and organic (quino-

neor anthraquinone,⁴ nitro aromatic,⁵ TTF⁶) centers into a variety of crown ether, aza crown ether, and cryptand macrocyclic structural frameworks and have shown some of these compounds to be selective and electrochemically responsive to the binding of cationic guest species.

The calixarenes are a family of synthetic macrocyclic receptors consisting of cyclic arrays of phenol moieties linked by methylene groups.⁷ They have been modified at the lower hydroxyl rim to produce a variety of novel ionophores for group 1 and 2,⁸ transition,⁹ and lanthanide¹⁰ metal cations, some of which have been utilized in potentiometric ion selective membrane electrodes.¹¹

* To whom correspondence should be addressed.

† University of Oxford.

‡ Present address: Department of Materials Science and Metallurgy, University of Cambridge, Pembroke St., Cambridge CB2 3QZ, U.K.

§ University of Reading.

|| Present address: School of Applied Chemistry, Curtin University of Technology, Perth, Western Australia.

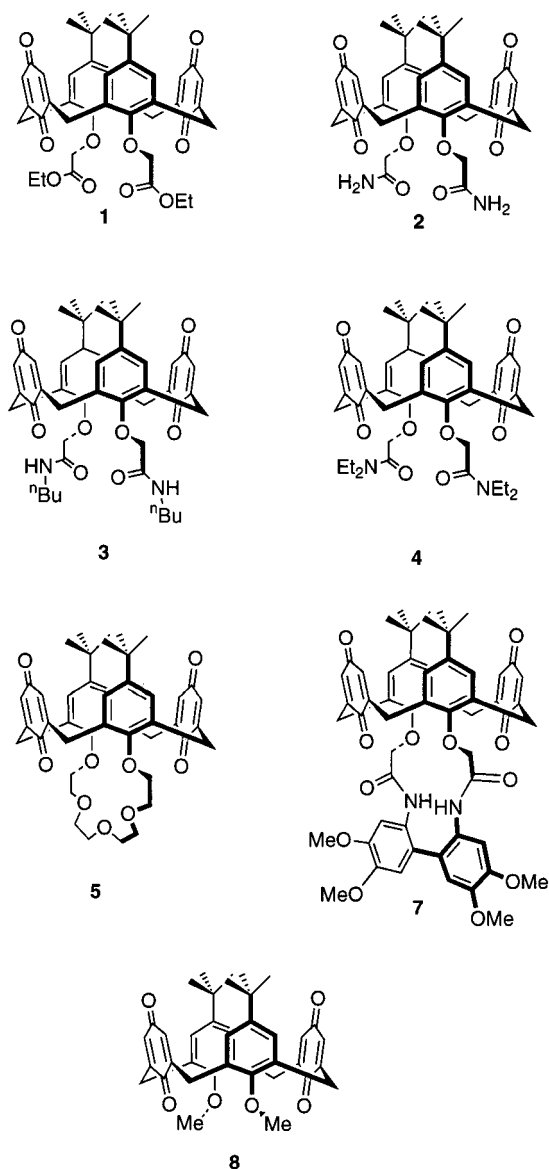
⊥ Cambridge Crystallographic Data Centre.

Ⓢ Abstract published in *Advance ACS Abstracts*, October 15, 1997.

- (1) (a) Kaifer, A.; Echegoyen, L. In *Cation Binding by Macrocyclic Systems*; Inoue, Y., Gokel, G. W., Eds.; Marcel Dekker: New York, 1990; p 363. (b) Beer, P. D. *Adv. Inorg. Chem.* **1992**, *39*, 79. (c) Beer, P. D. *Adv. Mater.* **1994**, *6*, 607. (d) Beer, P. D.; Gale, P. A.; Chen, Z. *Adv. Phys. Org. Chem.*, in press.
- (2) (a) Hall, C. D.; Sharpe, N. W.; Danks, I. P.; Sang, Y. P. *J. Chem. Soc., Chem. Commun.* **1989**, 419. (b) Fu, E.; Green, M. L. H.; Lowe, V. J.; Marder, S. R. *J. Organomet. Chem.* **1988**, *341*, C39. (c) Lowe, N. D.; Garner, C. D. *J. Chem. Soc., Dalton Trans.* **1993**, 2197. (d) van Veggel, F. C. J. M.; Harkema, S.; Bos, M.; Verboom, W.; Woolthuis, G. K.; Reinhoudt, D. N. *J. Org. Chem.* **1989**, *54*, 2351. (e) Hall, C. D.; Tucker, J. H. R.; Chu, S. Y. F.; Parkins, A. W.; Nyburg, S. C. *J. Chem. Soc., Chem. Commun.* **1993**, 1505. (f) Plenio, H.; Diodone, R. *Inorg. Chem.* **1995**, *34*, 3964. (g) Medina, J. C.; Goodnow, T. T.; Rojas, M. T.; Atwood, J. L.; Lynn, B. C.; Kaifer, A. E.; Gokel, G. W. *J. Am. Chem. Soc.* **1992**, *114*, 10583.

- (3) (a) Beer, P. D.; Kocian, O.; Mortimer, R. J.; Ridgway, C. *J. Chem. Soc., Dalton Trans.* **1993**, 2629. (b) Beer, P. D.; Chen, Z.; Ogden, M. I. *J. Chem. Soc., Faraday Trans.* **1995**, *91*, 295. (c) Beer, P. D.; Kocian, O.; Mortimer, R. J.; Ridgway, C.; Stradiotto, N. R. *J. Electroanal. Chem.* **1996**, *408*, 61.
- (4) (a) Delgado, M.; Gustowski, D. A.; Yoo, H. K.; Gatto, V. J.; Gokel, G. W.; Echegoyen, L. *J. Am. Chem. Soc.* **1988**, *110*, 119. (b) Gustowski, D. A.; Delgado, M.; Gatto, V. J.; Echegoyen, L.; Gokel, G. W. *J. Am. Chem. Soc.* **1986**, *108*, 7553. (c) Delgado, M.; Wolf, R. E., Jr.; Hartman, J. R.; McCafferty, G.; Yagbasan, R.; Rawle, S. C.; Watkin, D. J.; Cooper, S. R. *J. Am. Chem. Soc.* **1992**, *114*, 8983. (d) Bethell, D.; Dougherty, G.; Cupertino, D. C. *J. Chem. Soc., Chem. Commun.* **1995**, 675.
- (5) (a) Kaifer, A. E.; Echegoyen, L.; Gustowski, D. A.; Goli, D. M.; Gokel, G. W. *J. Am. Chem. Soc.* **1983**, *105*, 7168. (b) Kaifer, A. E.; Gustowski, D. A.; Echegoyen, L.; Gatto, V. J.; Schultz, R. A.; Cleary, T. P.; Morgan, C. R.; Goli, D. M.; Rios, A. M.; Gokel, G. W. *J. Am. Chem. Soc.* **1985**, *107*, 1958.
- (6) (a) Otsubo, T.; Ogura, F. *Bull. Chem. Soc. Jpn.* **1985**, *58*, 1343. (b) Jørgensen, T.; Hansen, T. K.; Becker, J. *Chem. Soc. Rev.* **1994**, 41 and references cited therein.
- (7) (a) Gutsche, C. D. *Calixarenes: Monographs in Supramolecular Chemistry*; Stoddart, J. F., Ed.; The Royal Society of Chemistry: Cambridge, U.K., 1989. (b) Böhmer, V. *Angew. Chem., Int. Ed. Engl.* **1995**, *34*, 713.

Chart 1. Calix[4]diquinone Ligands



Oxidation of the calixarene framework has produced a variety of calix[4]arene mono-, di-, tri-, and tetraquinone species¹² whose electrochemical properties have recently been described.¹³ Surprisingly, the cation coordination chemistry of the calixdiquinones and their potential use as prototype amperometric sensing molecules has not as yet been fully explored, although Echegoyen and co-workers have shown that there are marked perturbations of the quinone redox couples on addition of sodium cations.^{13a} We report here the synthesis of new lower rim ester, amide, and crown ether functionalized calix[4]-diquinone molecules (Chart 1) and their coordination and electrochemical recognition properties with group 1 and 2 metal, ammonium, and alkylammonium cations.¹⁴

Experimental Section

Solvent and Reagent Pretreatment. Dichloromethane and acetonitrile were distilled from CaH₂; diethyl ether was distilled from sodium wire. Triethylamine was dried over KOH. Column chromatography

was performed with silica gel (Merck, particle size 0.0015–0.040 nm). All reactions were carried out under a nitrogen atmosphere. Unless stated to the contrary, commercial grade chemicals were used without further purification.

Instrumentation. NMR spectra were obtained on a Bruker AM300 spectrometer using the solvent deuterium signal as an internal reference. Fast atom bombardment (FAB) mass spectrometry was performed by the EPSRC mass spectrometry service at the University of Wales, Swansea, Wales. Electrochemical measurements were carried out using an EG&G Princeton Applied Research 273 potentiostat/galvanostat. All reported voltammograms were recorded on the first potential sweep. Dichloromethane, acetonitrile, and mixtures of the two were used as solvents because of solubility, solution resistance, and literature comparison. The electrochemical cell was an unsealed one-compartment cell with a glassy-carbon disk (diameter 0.30 cm) working electrode, a Ag/Ag⁺ reference electrode, and a platinum-wire coil (length 10.0 cm) counter electrode. The reference contained an internal solution of 1.0 mM AgNO₃ and 0.1 M *n*-Bu₄NBF₄ in CH₃CN and was incorporated with a salt bridge containing 0.1 M *n*-Bu₄NBF₄ in the respective solvent. Once made, it showed a stable potential of 330 ± 10 mV vs SCE with shifting, ≤5 mV, under explored conditions. Argon, saturated with the appropriate solvent to minimize evaporation, was used at all times for solution degassing. A Kemet diamond compound spray (6.0 μm) was used to polish the working electrode followed by rinsing in water and then the respective solvent. The electrode was then dried by an air flow. Experiments were conducted at room temperature. A PC-controlled Hewlett-Packard HP 8452A diode array spectrophotometer was employed for recording the electronic absorption spectra. Titrations were conducted by adding a cation solution (0.1 M in CH₃CN or MeOH) using a 10 μL syringe to a cuvette containing 3.0 mL of compound solution (5 × 10⁻⁵ M in CH₂Cl₂/CH₃CN (4/21 (v/v)) or MeOH). All solutions contained 0.1 M tetrabutylammonium tetrafluoroborate as supporting electrolyte. The maximum addition for all the cations was less than 150 μL to minimize the change in solution volume. The spectrum was recorded after each addition. The titration data were processed using the SPECFIT global analysis program, which gave the calculated stability constants.¹⁵ Elemental analyses were carried out by the Inorganic Chemistry Laboratory Microanalytical Service. Samples were ground and dried under high vacuum prior to analysis.

(8) (a) Collins, E. M.; McKervey, M. A.; Madigan, E.; Moran, M. B.; Owens, M.; Ferguson, G.; Harris, S. J. *J. Chem. Soc., Perkin Trans. 1* **1991**, 3137 and references cited therein. (b) Arnaud-Neu, F.; Barrett, G.; Harris, S. J.; Owens, M.; McKervey, M. A.; Schwing-Weill, M.-J.; Schwinté, P. *Inorg. Chem.* **1993**, 32, 2644. (c) Dijkstra, P. J.; Brunink, J. A. J.; Bugge, K. E.; Reinhoudt, D. N.; Harkema, S.; Ungaro, R.; Ugozzoli, F.; Ghidini, E. *J. Am. Chem. Soc.* **1989**, 111, 7567.

(9) (a) Floriani, C.; Jacoby, D.; Chiesi-Villa, A.; Guastini, C. *Angew. Chem., Int. Ed. Engl.* **1989**, 28, 1376. (b) Moran, J. K.; Roundhill, D. M. *Inorg. Chem.* **1992**, 31, 4213. (c) Loeber, C.; Matt, D.; De Cian, A.; Fischer, J. *J. Organomet. Chem.* **1994**, 475, 297. (d) Beer, P. D.; Martin, J. P.; Drew, M. G. B. *Tetrahedron* **1992**, 48, 9917. (e) Regnoul de Vains, J.-B.; Lamartine, R. *Helv. Chim. Acta* **1994**, 77, 1817. (f) Beer, P. D.; Chen, Z.; Goulden, A. J.; Grieve, A.; Hesk, D.; Szemes, F.; Wear, T. *J. Chem. Soc., Chem. Commun.* **1994**, 1269.

(10) (a) Sabbatini, N.; Guardigli, M.; Mecati, A.; Balzani, V.; Ungaro, R.; Ghidini, E.; Casnati, A.; Pochini, A. *J. Chem. Soc., Chem. Commun.* **1990**, 878. (b) Sabbatini, N.; Guardigli, M.; Mannet, I.; Ungaro, R.; Casnati, A.; Fischer, C.; Ziessel, R.; Ulrich, G. *New J. Chem.* **1995**, 19, 137. (c) Rudkevich, D. M.; Verboom, W.; van der Tol, E.; van Staveren, C. J.; Kaspersen, F. M.; Verhoeven, J. W.; Reinhoudt, D. N. *J. Chem. Soc., Perkin Trans. 2* **1995**, 131. (d) Arnaud-Neu, F. *Chem. Soc. Rev.* **1994**, 235 and references cited therein. (e) Beer, P. D.; Drew, M. G. B.; Kan, M.; Leeson, P. B.; Ogden, M. I.; Williams, G. *Inorg. Chem.* **1996**, 35, 2202. (f) Beer, P. D.; Drew, M. G. B.; Grieve, A.; Kan, M.; Leeson, P. B.; Nicholson, G.; Ogden, M. I.; Williams, G. *Chem. Commun.* **1996**, 1117.

(11) Diamond, D.; McKervey, M. A. *Chem. Soc. Rev.* **1996**, 15.

(12) (a) Morita, Y.; Agawa, T.; Kai, Y.; Kanehisa, N.; Kasai, N.; Nomura, E.; Taniguchi, H. *Chem. Lett.* **1989**, 1349. (b) Morita, Y.; Agawa, T.; Nomura, E.; Taniguchi, H. *J. Org. Chem.* **1992**, 57, 3658. (c) Suga, K.; Fujihira, M.; Morita, Y.; Agawa, T. *J. Chem. Soc., Faraday Trans.* **1991**, 1575. (d) Reddy, P. A.; Kashyap, R. P.; Watson, W. H.; Gutsche, C. D. *Isr. J. Chem.* **1992**, 32, 89. (e) Reddy, P. A.; Gutsche, C. D. *J. Org. Chem.* **1993**, 58, 3245.

(13) (a) Gómez-Kaifer, M.; Reddy, P. A.; Gutsche, C. D.; Echegoyen, L. *J. Am. Chem. Soc.* **1994**, 116, 3580. (b) Bettge, H. C. Y.; Moutet, J. C.; Ulrich, G.; Ziessel, R. *J. Electroanal. Chem.* **1996**, 406, 247.

(14) Preliminary aspects of this work have been published previously: (a) Beer, P. D.; Chen, Z.; Gale, P. A. *Tetrahedron* **1994**, 50, 931. (b) Beer, P. D.; Chen, Z.; Drew, M. G. B.; Gale, P. A. *J. Chem. Soc., Chem. Commun.* **1994**, 2207. (c) Chen, Z.; Gale, P. A.; Heath, J. A.; Beer, P. D. *J. Chem. Soc., Faraday Trans.* **1994**, 2931.

(15) The computer program used to calculate the stability constants was SPECFIT v 2.02, Spectrum Software Associates, Chapel Hill, NC.

Synthesis. **5,17-Di-*tert*-butyl-26,28-bis(carboethoxymethoxy)calix[4]diquinone (1).** *p-tert*-Butylcalix[4]arene bis(ethyl ester)^{8a} (0.82 g, 1 mmol) was stirred in Ti(OCOCF₃)₃/trifluoroacetic acid solution (6.8 mL, 6 mmol) for 2 h in the dark.¹⁶ The trifluoroacetic acid was then removed *in vacuo* and the residue poured onto ice/water (50 mL). The product was extracted with chloroform (100 mL) and the extract then washed with water (100 mL). The organic layer was then dried over MgSO₄ and reduced *in vacuo*. The product was isolated by crystallization *via* slow evaporation from a mixture of methanol and dichloromethane. The orange crystals (0.48 g, 65%) were collected and dried *in vacuo*; mp 235 °C dec. ¹H NMR (CD₂Cl₂): δ 6.85 (s, 4H, Ar H), 6.71 (s, 4H, Qu H), 4.39 (s, 4H, OCH₂), 4.23 (q, ³J = 7.1 Hz, 4H, CH₂CH₃), 4.02 (d, ²J = 13.3 Hz, 4H, ArCH₂Qu, H_{ax}), 3.27 (d, ²J = 13.3 Hz, 4H, ArCH₂Qu, H_{eq}), 1.28 (t, ³J = 7.1 Hz, 6H, CH₂CH₃), 1.10 (s, 18H, (CH₃)₃C). ¹³C NMR (CD₂Cl₂): δ 188.57 (C=O), 185.40 (C=O), 169.26 (C=O), 147.86, 146.61, 132.88 (Ar H), 128.36, 126.81 (Qu H), 71.29 (CH₂O), 61.35 (CH₂O), 33.88 ((CH₃)₃C), 32.71 (ArCH₂Qu), 31.27 ((CH₃)₃C), 14.10 (CH₃CH₂). IR (KBr): 1760.0, 1733.9, 1654.8 cm⁻¹ (C=O). Anal. Calcd for C₄₄H₄₈O₁₀·H₂O: C, 70.0; H, 6.7. Found: C, 70.0; H, 6.7. FABMS: *m/z* 737 (MH⁺), 759 (MNa⁺), 869 (MCs⁺).

5,17-Di-*tert*-butyl-26,28-bis(carbamoylmethoxy)calix[4]diquinone (2). 5,11,17,23-Tetra-*tert*-butyl-25,27-bis(carbamoylmethoxy)-26,28-dihydroxycalix[4]arene^{8a} (2.0 g, 2.62 mmol) was stirred in 0.88 M Ti(OCOCF₃)₃/trifluoroacetic acid solution (17.9 mL, 0.88 M) for 2 h in darkness. The product was then extracted with chloroform (200 mL) and the extract washed with water (1000 mL). A solution of [2.2.1]cryptand (100 mg in 2 mL of CHCl₃) was added to the organic layer and the washing repeated. The organic layer was then washed with HCl solution (500 mL, 1.0 M) and then with water (100 mL). The organic layer was then reduced and dried *in vacuo*. The product was precipitated from dichloromethane/hexane as a yellow powder (1.01 g, 61%); mp 265 °C. ¹H NMR (CDCl₃): δ 8.02 (s, 2H, NH), 6.87 (s, 4H, Ar H), 6.74 (s, 4H, C=CH), 6.66 (s, 2H, NH), 5.29 (CH₂Cl₂), 4.31 (s, 4H, OCH₂), 3.98 (d, *J* = 13.0 Hz, 4H, ArCH₂Qu), 3.21 (d, *J* = 13.0 Hz, 4H, ArCH₂Qu), 1.10 (s, 18H, (CH₃)₃C). ¹³C NMR (CDCl₃): δ 187.87 (C(O)NH₂), 171.73, 150.99 (Ar H), 148.35 (C=O, coincident), 147.89, 132.48, 129.21 (Qu H), 126.70, 71.67 (OCH₂), 34.19 (CH₃)₃C, 31.59 (ArCH₂Qu), 31.10 ((CH₃)₃C). IR(KBr): 1610, 1656 cm⁻¹ (br). FABMS: *m/z* 678 (M⁺), 701 (MNa⁺). Anal. Calcd for C₄₀H₄₂O₈N₂·H₂O (sample recrystallized from ethanol/water): C, 68.95; H, 6.36; N, 4.02. Found: C, 68.13; H, 6.04; N, 3.73.

5,11,17,23-Tetra-*tert*-butyl-25,27-bis(*n*-butylcarbamoyl)methoxy)-26,28-dihydroxycalix[4]arene (9). *p-tert*-Butylcalix[4]arene bis(acid chloride)^{8a} (2.0 g, 2.6 mmol) was dissolved in dry CH₂Cl₂ (25 mL). *n*-Butylamine (0.46 g, 6.2 mmol) and Et₃N (0.66 g, 6.6 mmol) were dissolved in dry CH₂Cl₂ (25 mL) and added to the acid chloride solution, and the reaction mixture was stirred for 12 h. The solvents were removed *in vacuo*, and the product was precipitated from CH₂Cl₂/hexane as a white powder (1.0 g, 44%); mp 248–253 °C. ¹H NMR (CDCl₃): δ 8.85 (t, 2H, CONH), 7.63 (s, 2H, OH), 7.09 (s, 4H, Ar H), 6.94 (s, 4H, Ar H), 4.57 (s, 4H, OCH₂), 4.12 (d, ²J = 13.5 Hz, 4H, ArCH₂Ar, H_{ax}), 3.44 (d, *J* = 13.5 Hz, 4H, ArCH₂Ar, H_{eq}), 3.39 (m, 4H, CH₂), 1.61 (m, 4H, CH₂), 1.38 (m, 4H, CH₂), 1.27 (s, 18H, (CH₃)₃C), 1.05 (s, 18H, (CH₃)₃C), 0.91 (t, ³J = 7.3 Hz, 6H, CH₃CH₂). ¹³C NMR (CDCl₃): δ 167.96 (C=O), 149.37 (Ar), 148.81 (Ar), 148.46 (Ar), 143.19 (Ar), 132.25 (Ar), 127.20 (Ar), 126.18 (Ar H), 125.55 (Qu H), 74.82 (OCH₂), 39.21 (CH₂), 34.04 ((CH₃)₃C), 33.86 ((CH₃)₃C), 31.95 (CH₂), 31.53 ((CH₃)₃C), 31.22 (CH₂), 30.87 ((CH₃)₃C), 20.15 (CH₂), 13.62 (CH₃CH₂). IR (KBr): 1680.0 cm⁻¹ (C=O). FABMS: *m/z* 876 (MH⁺), 898 (MNa⁺), 914 (MK⁺). Anal. Calcd for C₅₆H₇₈N₂O₆: C, 76.85; H, 8.98; N, 3.20. Found: C, 75.82; H, 9.20; N, 2.81.

5,17-Di-*tert*-butyl-26,28-bis(*n*-butylcarbamoyl)methoxy)calix[4]diquinone (3). Compound **9** (0.80 g, 0.92 mmol) was stirred in Ti(OCOCF₃)₃/trifluoroacetic acid solution (6.3 mL/0.88 M) for 2 h in the dark. The trifluoroacetic acid was then removed *in vacuo* and the residue poured onto ice/water (50 mL). The product was then extracted with chloroform (100 mL) and the extract washed with water (100 mL). The organic layer was then dried over MgSO₄ and reduced *in vacuo*. The product was precipitated from dichloromethane as a yellow powder

(0.47 g, 65%); mp 255 °C (dec). ¹H NMR (CDCl₃): δ 8.25 (br t, 2H, CONH), 7.63 (s, 2H, OH), 6.82 (s, 4H, Ar H), 6.69 (s, 4H, Qu H), 4.28 (s, 4H, OCH₂), 4.03 (d, ²J = 12.9 Hz, 4H, ArCH₂Qu, H_{ax}), 3.43 (m, 4H, CH₂), 3.15 (d, ²J = 12.9 Hz, 4H, ArCH₂Qu, H_{eq}), 1.60 (m, 4H, CH₂), 1.41 (m, 4H, CH₂), 1.08 (s, 18H, (CH₃)₃C), 0.94 (t, 6H, CH₃CH₂). ¹³C NMR (CDCl₃): δ 187.82 (C=O), 185.79 (C=O), 168.79 (C=O), 151.53 (Ar), 148.44 (Ar), 147.88, 132.42 (Ar H), 128.95 (Ar), 126.63 (Ar H), 72.61 (OCH₂), 39.11 (CH₂), 34.15 ((CH₃)₃C), 31.48 (CH₂), 31.74 ((CH₃)₃C), 30.90 (CH₂), 20.14 (CH₂), 13.74 (CH₃CH₂). IR (KBr): 1656, 1678 cm⁻¹ (C=O). FABMS: *m/z* 791 (MH⁺), 813 (MNa⁺), 967 (MH⁺NOBA). Anal. Calcd for C₄₈H₅₈N₂O₈: C, 72.89; H, 7.39; N, 3.54. Found: C, 72.74; H, 7.47; N, 3.55.

5,17-Di-*tert*-butyl-26,28-bis((diethylcarbamoyl)methoxy)calix[4]diquinone (4). 5,11,17,23-Tetra-*tert*-butyl-25,27-bis((diethylcarbamoyl)methoxy)-26,28-dihydroxycalix[4]arene^{8a} (1.0 g, 1.18 mmol) was stirred in Ti(OCOCF₃)₃/trifluoroacetic acid solution (8.1 mL, 7.1 mmol) for 2 h in the dark. The trifluoroacetic acid was then removed *in vacuo* and the residue poured onto ice/water (50 mL). The product was extracted with chloroform (100 mL) and the extract washed with 100 mL of water. The organic layer was then dried over MgSO₄ and reduced *in vacuo*. The residue was purified by column chromatography on silica gel with chloroform/methanol (90/10) as eluent and the product isolated as a brown glassy solid (0.12 g, 13%); mp 195 °C. ¹H NMR (CDCl₃): δ 6.86 (s, 4H, Ar H), 6.62 (s, 4H, Qu H), 5.31 (CH₂Cl₂), 4.35 (s, 4H, OCH₂), 3.66 (d, ²J = 13.3 Hz, 4H, ArCH₂Qu, H_{ax}), 3.44 (m, 4H, NCH₂CH₃), 3.32 (d, ²J = 13.3 Hz, 4H, ArCH₂Qu, H_{eq}), 1.28 (m, 12H, NCH₂CH₃), 1.13 (s, 18H, (CH₃)₃C). ¹³C NMR (CDCl₃): δ 188.59 (C=O), 185.47 (C=O), 167.17 (CONH), 147.66, 146.62, 132.53 (Ar H), 128.89, 127.21 (Qu H), 73.57 (CH₂O), 61.35 (CH₂O), 41.97 (CH₃CH₂), 40.29 (CH₃CH₂), 34.04 ((CH₃)₃C), 33.18 (ArCH₂Qu), 31.34 ((CH₃)₃C), 14.44 (CH₃CH₂), 12.61 (CH₃CH₂). IR(KBr): 1657 cm⁻¹ (br, C=O). FABMS: *m/z* 813 (MNa⁺), 923 (MCs⁺). Anal. Calcd for C₄₈H₅₈N₂O₈·CH₂Cl₂: C, 67.19; H, 6.90; N, 3.20. Found: C, 67.33; H, 6.86; N, 3.18.

5,17-Di-*tert*-butyl-26,28-(crown-5)calix[4]diquinone (5). *p-tert*-Butylcalix[4]arene-crown-5¹⁷ (1.4 g, 1.75 mmol) was stirred in Ti(OCOCF₃)₃/trifluoroacetic acid solution (11.76 mL, 0.88 M) for 2 h in the dark. The trifluoroacetic acid was then removed *in vacuo* and the residue poured onto ice/water (50 mL). The product was then extracted with chloroform (200 mL) and the extract washed with water (1000 mL). A solution of [2.2.1]cryptand (25 mg in 0.5 mL of CH₃CN) was added to the organic layer and the washing repeated. The organic layer was washed with HCl solution (200 mL, 1.0 M) and then with water (100 mL). The organic layer was then reduced and dried *in vacuo*. The product was precipitated from dichloromethane/hexane as a yellow powder (0.41 g, 33%); mp 250 °C dec. ¹H NMR (CDCl₃): δ 6.90 (s, 4H, Ar), 6.63 (s, 4H, C=CH), 5.30 (CH₂Cl₂), 3.8–4.15 (m, 16H, OCH₂CH₂O and QuCH₂Ar, H_{ax}), 3.61 (t, 4H, OCH₂), 3.31 (d, ²J = 13 Hz, 4H, ArCH₂Qu, H_{eq}), 1.15 (s, 18H, (CH₃)₃C). ¹³C NMR (CDCl₃): δ 188.61 (C=O), 185.44 (C=O), [153.51, 147.85, 146.28 Ar/Qu], 132.52 (Qu/Ar H), 129.53 (Ar), 127.15 (Qu/Ar H), [69.99, 70.27, 70.95, 72.66 (OCH₂)], 34.03 ((CH₃)₃C), 33.40 (QuCH₂Ar), 31.36 ((CH₃)₃C). IR (KBr): 1629, 1654 cm⁻¹ (C=O). FABMS: *m/z* 745 (MNa⁺), 761 (MK⁺). Anal. Calcd for C₄₄H₅₀O₉·0.5CH₂Cl₂: C, 69.84; H, 6.72. Found: C, 70.34; H, 6.70.

5,11,17,23-Tetra-*tert*-butyl-25,27-bis(((3,4-dimethoxyphenyl)carbamoyl)methoxy)calix[4]arene (6). *p-tert*-Butylcalix[4]arene bis(acid chloride)^{8a} (1.6 g, 2.1 mmol) was dissolved in dry CH₂Cl₂ (25 mL). 4-Aminoveratrole (0.67 g, 4.4 mmol) and Et₃N (0.60 g, 6 mmol) were dissolved in dry CH₂Cl₂ (50 mL), and this mixture was added to the acid chloride solution. The reaction mixture was stirred for 12 h and washed with water (2 × 100 mL) and the organic layer separated and dried over MgSO₄. The solvent was removed *in vacuo*, and the product was precipitated from CH₂Cl₂/hexane as a white powder (0.84 g, 39%). ¹H NMR (CDCl₃): δ 10.12 (2H, s, CONH), 8.16 (2H, s, ArOH), 7.36 (2H, s, Ar H), 7.14 (4H, s, Ar H), 7.01 (4H, s, Ar H), 6.85 (2H, d, *J* = 8.2 Hz, ArH), 6.73 (2H, d, *J* = 8.6 Hz, ArH), 4.61 (4H, s, CH₂NH), 4.22 (4H, d, *J* = 13.3 Hz, ArCH₂Ar), 3.88 (6H, s, ArOCH₃), 3.74 (6H, s, ArOCH₃), 3.53 (4H, d, *J* = 13.3 Hz, ArCH₂Ar), 1.29 (18H, s, (CH₃)₃C), 1.09 (18H, s, (CH₃)₃C). ¹³C NMR

(CDCl₃): δ 165.77, 149.98, 149.87, 148.20, 145.19, 145.03, 144.00, 140.63, 134.74, 132.21, 127.81, 126.41, 126.01, 124.62, 123.31, 74.21, 56.41, 56.07, 34.27, 34.07, 32.61, 31.59, 31.04. FABMS m/z 1036 (MH⁺). Anal. Calcd for C₆₄H₇₈N₂O₁₀·CH₂Cl₂: C, 69.69; H, 7.20; N, 2.50. Found: C, 69.87; H, 6.44; N, 2.71.

5,17-Di-*tert*-butyl-26,28-((3,3',4,4'-tetramethoxy-5,5'-biphenyl)-carbamoyl)methoxycalix[4]diquinone (7). Compound **6** (0.93 g, 0.90 mmol) was stirred with Ti(OACF₃)₃/trifluoroacetic acid (6.14 mL, 0.88 M) for 2 h in the dark. The trifluoroacetic acid was then removed *in vacuo* and the residue poured onto ice/water (50 mL). The product was extracted with chloroform (100 mL) and washed with 100 mL of water. The organic layer was then dried over MgSO₄ and reduced *in vacuo*. The residue was purified by column chromatography on silica gel with chloroform/methanol (90/10) as eluent. The product was the first band from the column and was collected and reduced *in vacuo*. The solid was recrystallized from dichloromethane/hexane, producing red crystals (75 mg, 9%); mp 245–250 °C dec. ¹H NMR (CD₂Cl₂): δ 10.70 (s, 2H, CONH), 7.15 (d, ²J = 2.2 Hz, 2H, Ar H), 7.09 (d, ²J = 2.2 Hz, 2H, Ar H), 7.03 (s, 2H, Ar H), 6.76 (s, 2H, Ar H), 6.72 (s, 2H, Qu H), 6.71 (s, 2H, Qu H), 4.46 (d, ²J = 14.8 Hz, 2H, OCH₂), 4.32 (d, ²J = 12.3 Hz, 2H, ArCH₂Ar, H_{ax}), 4.21 (d, ²J = 12.1 Hz, 2H, ArCH₂Ar, H_{ax}), 3.97 (d, ²J = 14.8 Hz, 2H, OCH₂), 3.92 (s, 6H, OMe), 3.61 (s, 6H, OMe), 3.23 (d, ²J = 12.3 Hz, 2H, ArCH₂Ar, H_{eq}), 3.11 (d, ²J = 12.1 Hz, 2H, ArCH₂Ar, H_{eq}), 1.20 (s, 18H, (CH₃)₃C). ¹³C NMR(CDCl₃): δ 187.25 (C=O), 186.02 (C=O), 166.68 (CONH), [148.14, 148.62, 148.76, 149.34, 151.70 (Ar)], 133.55 (Ar H), 133.13 (Ar H), [130.16, 130.63, 131.51 (Ar)], 127.47 (Ar H), 126.02, 114.04 (Qu H), 110.62 (Qu H), 73.00 (OCH₂), 56.46 (OCH₃), 56.13 (OCH₃), 34.50 (CH₃C), 31.26 (CH₃C), 29.63 (ArCH₂Qu). IR (KBr): 1609, 1657, 1694 cm⁻¹ (C=O). FABMS: m/z 949 (MH⁺), 971 (MNa⁺). Anal. Calcd for C₅₆H₅₆N₂O₁₂·CH₂Cl₂: C, 68.56; H, 5.85; N, 2.81. Found: C, 68.37; H, 5.93; N, 2.68.

Cation Complexes. For all complexes formed, an excess of the cation salt in ethanol was added to a solution of the ligand in dichloromethane and the mixture filtered through a cotton wool plug. Care was taken with the isolation of perchlorate salts of the calixdiquinone-metal complexes, as they are explosive. In all cases, the complexes were isolated in small quantities only.¹⁸ The solution was then allowed to slowly evaporate, and the complex crystallized out. The compounds were characterized by elemental analysis (after exposure to high vacuum for typically 2 days),¹⁹ NMR spectroscopy, and X-ray crystallography.

Ammonium Complex of 1. Anal. Calcd for C₄₄H₄₈O₁₀–NH₄PF₆·0.25(CH₂Cl₂·EtOH): C, 57.63; H, 5.84; N, 1.50. Found: C, 57.68; H, 5.86; N, 1.57. ¹H NMR (CDCl₃): δ [7.06, 7.26, 7.41 br, 4H, NH₄⁺], 6.71 (s, 4H, Qu H), 6.67 (s, 4H, Ar H), 5.30 (s, trace quantity, CH₂Cl₂), 4.35 (s, 4H, OCH₂) (partially coincident), 4.32 (q, ³J = 7.1 Hz, 4H, CH₂CH₃), 4.17 (d, ²J = 13.0 Hz, 4H, ArCH₂Qu, H_{ax}), 3.72 (q, ³J = 6.9 Hz, trace quantity, CH₂ ethanol), 3.06 (d, ²J = 13.0 Hz, 4H, ArCH₂Qu, H_{eq}), 1.34 (t, ³J = 7.2 Hz, 6H, CH₂CH₃), 1.25 (t, ³J = 6.9 Hz, trace quantity, CH₃ ethanol), 0.99 (s, 18H, (CH₃)₃C).

Potassium Complex of 1. Anal. Calcd for C₄₄H₄₈O₁₀–KClO₄·0.5CH₂Cl₂: C, 58.23; H, 5.38; K, 4.26. Found: C, 58.50; H, 5.37; K, 4.27. Dichloromethane was not located in the crystal structure; however, a ¹H NMR spectrum in CDCl₃/CH₃CN did reveal the presence of trace amounts of the solvent. ¹H NMR (CDCl₃/CD₃CN (5/1 (v/v))): δ 6.88 (s, 4H, Ar H), 6.71 (s, 4H, Qu H), 5.34 (CH₂Cl₂ trace quantity), 4.32 (s, 4H, OCH₂), 4.20 (q, 4H, CH₂CH₃), 3.90 (d, 4H, ArCH₂Qu, H_{ax}), 3.25 (d, 4H, ArCH₂Qu, H_{eq}), 1.27 (t, 6H, CH₂CH₃), 1.07 (s, 18H, (CH₃)₃C).

Strontium Complex of 1. Anal. Calcd for C₄₄H₄₈O₁₀–Sr(ClO₄)₂·CH₂Cl₂: C, 48.77; H, 4.55; Sr, 7.91. Found: C, 49.11; H, 4.60; Sr, 7.33.

Sodium Complex of 2. The sodium complex was formed by dissolving the calixdiquinone in methanol and adding an excess of NaClO₄ in methanol. Crystallization occurred upon slow evaporation of the solvent. The crystals were then washed in methanol, ground, and exposed to high vacuum for 2 days. Anal. Calcd for

C₄₀H₄₂O₈N₂–NaClO₄: C, 59.96; H, 5.28; N, 3.50; Na, 2.87. Found: C, 56.69; H, 4.72; N, 3.18; Na, 3.03.

***n*-Butylammonium Complex of 4.** The *n*-butylammonium complex was formed by dissolving the calixdiquinone in dichloromethane and adding an excess of *n*-BuNH₃BF₄ in ethanol. Crystallization occurred upon slow evaporation of the solvent mixture. The crystals were then washed in ethanol, ground, and exposed to high vacuum for 2 days. Anal. Calcd for C₄₈H₅₈N₂O₈–*n*-BuNH₃BF₄·H₂O: C, 64.39; H, 7.48; N, 4.33. Found: C, 64.08; H, 7.52; N, 4.11.

Sodium Complex of 5. Anal. Calcd for C₄₄H₅₀O₉–NaOCOCF₃: C, 64.58; H, 6.06. Found: C, 64.33; H, 5.87.

Potassium Complex of 5. Anal. Calcd for C₄₄H₅₀O₉–KClO₄: C, 61.35; H, 5.85; K, 4.54. Found: C, 61.25; H, 5.72; K, 4.04.

Crystal Structure Determinations. Crystal data for all 10 structures are given in Table 1, together with refinement details. Nine sets of data were collected with Mo K α radiation using the MARresearch image plate system. The crystals were positioned at 75 mm from the image plate. A total of 95 frames were measured at 2° intervals with a counting time of 2 min. Data analyses were carried out with the XDS program.²⁰ The set of data for **1**-KClO₄ was collected with Mo K α radiation using an R-Axis image plate detector. The crystal to detector distance was set at 80 mm. For **1**-KClO₄, 120 frames were measured at 1.5° intervals with exposure times of 3 min per frame. The data were reduced with the R-Axis processing program.²¹

The structures of **1**-Sr(ClO₄)₂ and **5**-KClO₄ were solved by heavy-atom methods. The structure of **1**-KClO₄ was solved by direct methods with automatic structure rebuilding using SIR92,²² while all the other structures were determined by direct methods, using SHELXS-86.²³ Default refinement procedures were as follows. Non-hydrogen atoms were refined with anisotropic thermal parameters. Hydrogen atoms were included in geometric positions and given thermal parameters equivalent to 1.2 times those of the atom to which they were attached. The structures were refined on F^2 using SHELXL-93.²⁴ All calculations were carried out on a Silicon Graphics R4000 Workstation at the University of Reading. Exceptions and additions to this default procedure for individual structures are noted below.

Compound **1** has crystallographic C₂ symmetry. In **1**-Sr(ClO₄)₂ the *tert*-butyl groups and terminal ethyl groups had large thermal motion but no disordered model could be found. There was a large amount of disordered solvent in the lattice, and this was identified and refined as one dichloromethane with 50% occupancy and four water molecules each with 50% occupancy. In addition there was an acetonitrile molecule, but although it was coordinated to the metal atom, it was present only with 50% occupancy. In **1**-KClO₄, high thermal motion was found in the perchlorate anion but no suitable disordered model could be found. **1**-KClO₄ was refined on F using the Crystals program.²⁵ Calculations on this structure were carried out on a Silicon Graphics Workstation at the Cambridge Crystallographic Data Centre. In **2** there were 3.5 water molecules in the asymmetric unit. These were included in the refinement with full occupancy, but their hydrogen atoms could not be located. High thermal motion for the *tert*-butyl groups was observed, but no disordered model proved satisfactory.

In **2**-Na(ClO₄) the *tert*-butyl groups had high thermal motion but no suitable disordered model could be found. Four methanol molecules were located and given 50% occupancy.

In **4**-*n*-BuNH₃BF₄ there were two calix[4]diquinone molecules in the unit cell, together with two butylammonium cations and two disordered tetrafluoroborates. For the first anion, two sets of tetrahedral fluorines were located; for the second anion, two superimposed BF₄ anions were located and refined. All disordered atoms were given 50% occupancy and common thermal parameters with other atoms in the moiety. There was also a water molecule in the lattice, and this was given 50% occupancy. In **5**-Na(CF₃CO₂), the two *tert*-butyl groups

(18) Wolsey, W. C. *J. Chem. Educ.* **1973**, *50*, A335.

(19) It has been noted in the literature that elemental analysis of calixarene-containing compounds frequently produces erroneous results. For examples see: (a) Gutsche, C. D.; See, K. A. *J. Org. Chem.* **1992**, *57*, 4527. (b) Böhmer, V.; Jung, K.; Schön, M.; Wolff, A. *J. Org. Chem.* **1992**, *57*, 790.

(20) Kabsch, W. *J. Appl. Crystallogr.* **1988**, *21*, 916.

(21) R-Axis data reduction program; Molecular Structure Corp., The Woodlands, TX.

(22) Altomare, A.; Cascarano, G.; Giacovazzo, C.; Guagliardi, A. *J. Appl. Crystallogr.* **1993**, *26*, 343.

(23) Sheldrick, G. M. SHELXS-86. *Acta Crystallogr.* **1990**, *A46*, 467.

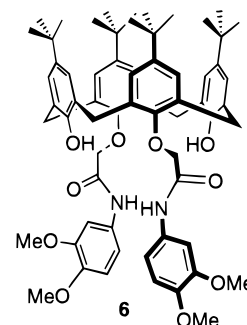
(24) Sheldrick, G. M. SHELXL-93, Program for Crystal Structure Refinement; University of Göttingen, Göttingen, Germany, 1993.

(25) Watkin, D. J.; Carruthers, R. J.; Betteridge, P. Crystals; Chemical Crystallography Laboratory: Oxford, U.K., 1985.

Table 1. Crystal Data for the 10 Structures

structure	1	2	4- <i>n</i> -Bu _n H ₃ BF ₄	5-Na(CF ₃ CO ₂) 0.5CH ₂ Cl ₂	5-KClO ₄ 0.5CH ₂ Cl ₂	7	8
solvent (if any)	1-Sr(ClO ₄) ₂ 0.5CH ₂ Cl ₂ , 0.5NCMe, 2H ₂ O	3.5H ₂ O	0.25H ₂ O	0.5CH ₂ Cl ₂	0.5CH ₂ Cl ₂	CH ₂ Cl ₂ , 2.5MeOH, 2.5H ₂ O	
empirical formula	C ₄₄ H ₄₈ O ₁₀	C ₄₀ H ₄₉ N ₂ O _{11.5}	C ₅₂ H _{70.5} BF ₄ N ₃ O _{8.25}	C _{46.5} H ₃₃ ClF ₃	C ₄₄ H ₅₀ ClKO ₃	C _{59.5} H ₆₇ Cl ₂ N ₂ O ₁₇	C ₃₈ H ₄₀ O ₆
fw	736.82	742.6	956.42	883.2	861.4	1153.1	592.6
cryst syst	orthorhombic	monoclinic	monoclinic	triclinic	triclinic	monoclinic	monoclinic
space group	Cmc2 ₁ (No. 36)	C2/c (No. 15)	P2 ₁ /c (No. 14)	P1 (No. 2)	P1 (No. 2)	P2 ₁ /n (No. 14)	C2/m (No. 12)
unit cell dimens							
<i>a</i> (Å)	14.158(10)	41.83(3)	18.01(2)	11.595(11)	11.649(11)	15.841(10)	15.619(7)
<i>b</i> (Å)	11.993(10)	10.973(9)	24.96(3)	14.288(13)	14.358(14)	22.475(17)	14.652(7)
<i>c</i> (Å)	22.029(15)	17.04(2)	25.48(3)	16.43(2)	16.38(2)	18.120(10)	16.206(8)
<i>α</i> (deg)	(90)	80.14(1)	(90)	71.06(1)	77.01(1)	(90)	(90)
<i>β</i> (deg)	(90)	80.40(1)	(90)	83.70(1)	77.86(1)	99.16(1)	117.65(1)
<i>γ</i> (deg)	(90)	88.85(1)	(90)	84.09(1)	72.64	(90)	(90)
<i>V</i> (Å ³)	3741	7713	10981	2514	2470	6369	3285
<i>T</i> (°C)	25	25	25	25	25	25	25
wavelength (Å)	0.710 73	0.710 73	0.710 73	0.710 73	0.710 73	0.710 73	0.710 73
<i>Z</i>	4	8	8	2	2	4	4
density (calc) (Mg/m ³)	1.308	1.272	1.157	1.167	1.158	1.203	1.198
abs coeff (mm ⁻¹)	0.092	0.094	0.086	0.148	0.218	0.167	0.079
final <i>R</i> indices ^a (<i>I</i> > 2σ(<i>I</i>))							
<i>R</i> ₁	0.0677	0.0952	0.1377	0.0826	0.0906	0.0935	0.0706
<i>wR</i> ₂	0.1662	0.2563	0.3688	0.2262	0.2242	0.2332	0.2204
<i>R</i> indices (all data)							
<i>R</i> ₁	0.0832	0.1358	0.1766	0.1438	0.1361	0.1427	0.1223
<i>wR</i> ₂	0.1769	0.2584	0.4031	0.3252	0.3172	0.2821	0.2999

$${}^a R_1 = \sum |F_o| - |F_c| / \sum |F_o|; wR_2 = [\sum w(F_o^2 - F_c^2) / \sum w(F_o^2)]^{1/2}; {}^b wR_1 = \sum w(|F_o| - |F_c|) / \sum w(F_o)$$



p-*tert*-Butylcalix[4]diquinone bis(methyl ether) **8**, which had previously been prepared by Gutsche and co-workers, was synthesized for use as a model compound in the subsequent coordination studies.^{12d}

Solid-State Structures of Host Compounds. Crystallographic data for all ten structures reported in this paper are shown in Table 1. The structures have a common numbering scheme, which is shown in Chart 2. Substituents at the lower rim in the other compounds continue numerically C(155), C(355), etc. The aromatic rings are denoted 1 and 3 and the quinone rings as 2 and 4. Conformations of the calix[4]-

were disordered, and two sets of three carbon atoms (with 50% occupancy) were included for each. The CF₃ group of the anion was disordered and two sets of three fluorine atoms were included with occupancies of 50%. There was also a disordered dichloromethane in the asymmetric unit. In **5-K(ClO₄)** the two *tert*-butyl groups had high thermal motion but no disordered model could be found. In **7** there was one solvent dichloromethane molecule with full occupancy together with five methanol and five water molecules, all with 50% occupancy. The hydrogen atoms on the dichloromethane and methanol molecules were included, but not those of the water molecules. Compound **8** has crystallographic *m* symmetry. Both *tert*-butyl groups were disordered around the mirror planes, and two sets were refined with half-occupancy. Hydrogen atoms on these groups were not included.

Results and Discussion

Synthesis. Using the methodology of McKillop and co-workers,¹⁶ which was first applied to calixarenes by Gutsche and co-workers,^{12d} a series of ionophoric *p*-*tert*-butylcalix[4]-diquinone species have been prepared from known lower-rim 1,3-bis-substituted calix[4]arenes. Oxidation of *p*-*tert*-butylcalix[4]arene bis(ethyl ester)^{8a} with Tl(OCOCF₃)₃ in trifluoroacetic acid gave the new *p*-*tert*-butylcalix[4]diquinone bis(ethyl ester) **1** in 65% yield. Similarly, oxidation of primary,^{8a} secondary, and tertiary^{8a} bis(amide)-substituted *p*-*tert*-butylcalix[4]arenes gave compounds **2–4** in 61%, 65%, and 13% respective yields.

A novel *p*-*tert*-butylcalixdiquinone–crown-5 molecule (**5**) was synthesized in 33% yield by an analogous oxidative procedure from the corresponding *p*-*tert*-butylcalix[4]arene crown ether compound.¹⁷

Thallium trifluoroacetate has been shown by McKillop to also cause the oxidative dehydrodimerization of aromatic groups by both inter-²⁶ and intramolecular²⁷ pathways, probably *via* the formation of a radical cationic intermediate. This synthetic methodology allows the synthesis of a bridged calixdiquinone to be achieved in one step from the aromatic-substituted nonbridged calixarene. The condensation of *p*-*tert*-butylcalix[4]arene bis(acid chloride) with 4-aminoveratrole in the presence of triethylamine gave the bis(veratrole)-substituted calix[4]arene **6**. Oxidation of **6** produced the new chiral bridged calixdiquinone **7** in 10% yield.

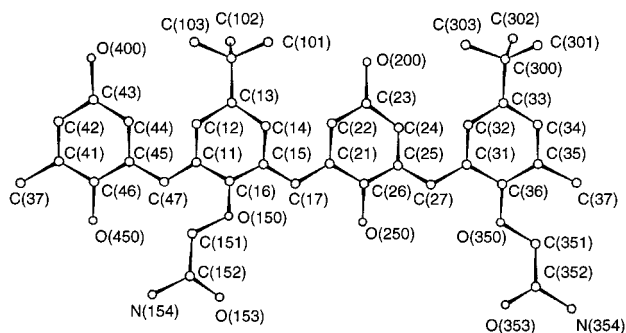
(26) McKillop, A.; Turrell, A. G.; Young, D. W.; Taylor, E. C. *J. Am. Chem. Soc.* **1980**, *102*, 6504.

(27) Taylor, E. C.; Andrade, J. G.; Rall, G. J. H.; McKillop, A. *J. Am. Chem. Soc.* **1980**, *102*, 6513.

Table 2. Conformations of the Calix[4]diquinones

structure	rings ^a				conformn
	1	2	3	4	
1	32.9(1)	105.5(2)	32.9(1)	105.5(2)	cone, quinone rings perpendicular ^b
1-Sr(ClO₄)₂	79.8(3)	37.4(3)	81.4(3)	38.4(3)	cone, aromatic rings perpendicular ^b
1-K(ClO₄)	94.5(4)	32.8(4)	89.5(4)	27.2(4)	cone, aromatic rings perpendicular ^b
2	83.7(1)	83.9(1)	89.7(1)	80.2(1)	1,3-alternate
2-Na(ClO₄)	80.8(3)	31.5(3)	78.8(3)	46.1(3)	cone, aromatic rings perpendicular ^b
4-<i>n</i>-BuNH₃BF₄	85.6(3)	23.9(2)	88.9(3)	28.4(5)	cone, aromatic rings perpendicular ^b
	82.8(4)	36.8(5)	89.0(3)	27.1(3)	cone, aromatic rings perpendicular ^b
5-Na(CF₃CO₂)	85.7(2)	32.3(2)	78.9(2)	38.0(3)	cone, aromatic rings perpendicular ^b
5-KClO₄	86.0(2)	31.4(2)	79.4(2)	40.4(2)	cone, aromatic rings perpendicular ^b
7	65.3(2)	56.6(3)	66.5(2)	54.8(2)	cone, regular
8	86.8(1)	93.1(1)	22.3(1)	93.1(1)	partial cone, aromatic ring unique

^a Angles >90° indicate that upper rim carbon atoms are closer to each other than are lower rim carbon atoms. Least-squares planes are calculated. Angles (deg) between the individual phenyl rings and the plane of the four methylene carbon atoms are given. Rings 1 and 3 are aromatic; rings 2 and 4 are quinones. ^b Perpendicular to the plane of the methylene carbon atoms.

Chart 2

diquinones can best be described by the angles between the rings and the plane of the four methylene groups C(17), C(27), C(37), and C(47), and these are listed in Table 2.

Compound **1** adopts the cone conformation in the solid state. There is a crystallographic C_2 axis such that the opposite rings take up similar orientations with respect to the methylene plane (Figure 1a). In this case the quinone rings are near-perpendicular to the plane (105.5(2)°) while the aromatic rings are near-horizontal (angles 32.9(1)°). This difference is unusual, as the disparity between orientations is typically found to have the opposite sense with the aromatic rings near-perpendicular and the quinone rings near-horizontal.

Compound **2** (Figure 1b) has the less common 1,3-alternate conformation, in which all four rings are perpendicular to the methylene plane (83.7(1), 83.9(1), 89.7(1), 80.2(1)°) but adjacent rings are oriented in opposite directions. While this conformation has been characterized for the calix[4]arenes,²⁸ this is the first example of a calix[4]diquinone adopting such a conformation. It seems likely in this case that the conformation is stabilized by the inclusion of a water molecule in the cavity. The figure shows the water molecule OW(1), which is hydrogen bonded to N(354) at 2.908(6) Å and O(150) at 3.108(5) Å. In contrast to N(354), which is directed toward the cavity at the lower rim of the calixdiquinone, N(154) is directed outward and forms two hydrogen bonds to solvent water molecules (as does O(353)). The adoption of a 1,3-alternate conformation forms a hydrophilic side to the molecule and a hydrophobic side. There are no solvent molecules at the hydrophobic side. Two molecules are connected at the hydrophilic end *via* two intermolecular hydrogen bonds between O(200) and N(354) of 3.04(5) Å around a 2-fold axis (Figure 2). Hydrogen-bonding distances are given in Table 3.

In compound **7**, a biphenyl moiety bridges the lower rim of the calixdiquinone via amide bonds to the 1- and 3-positions at

the lower rim (Figure 1c). The angle between the phenyl rings is 54.9(2)°. It is interesting that, in this compound, the calixarene rings all make similar angles with the methylene plane (65.3(2), 56.6(3), 66.5(2), 54.8(2)°). This unusual regularity could be due to the bridging biphenyl group, which rigidifies the structure, and also to the formation of intramolecular hydrogen bonds between the amide nitrogen atoms and the quinone oxygen atoms at the lower rim. The distances are N(154)–O(450) = 2.840(11) Å and N(354)–O(250) = 3.028(10) Å.

In contrast to the above structures, the conformation of compound **8** (Figure 1d) is an aryl partial cone in which one aromatic ring is directed downward (angle with methylene plane 86.8(1)°). As is usually the case, the opposite ring is near-horizontal to the methylene plane (22.3(1)°) while the two quinone rings are near-perpendicular (93.1(1)°). The molecule has crystallographic mirror symmetry, with the plane passing through the two aromatic rings. This partial cone conformation is also found in the analogous diethoxy compound.²⁹ Two other calix[4]diquinone structures have been determined to possess a partial cone conformation (including a dimethoxy derivative),²⁰ but these are unsubstituted at the upper rim. The dimethoxy compound also adopts an “aryl partial cone” conformation; however, the diisopropoxy derivative structure reported by Casnati et al. adopts a “quinone partial cone” conformation where one quinone ring is directed downward.

Variable-Temperature ¹H NMR Studies. The room-temperature ¹H NMR spectrum of **1** exhibits the typical AB splitting pattern of the ArCH₂Qu protons consistent with a cone conformation for the calixarene. However, low-temperature ¹H NMR spectra in dichloromethane-*d*₂ (Figure 3) revealed that, on cooling, the proton resonances of compound **1** broaden while the *tert*-butyl resonances split into two peaks. This suggests the presence of two species in solution: cone and partial cone conformers.

Ungaro and co-workers²⁹ also investigated the conformational properties of alkyl-substituted calixdiquinones and reported similar dynamic processes. A possible explanation for these variable-temperature ¹H NMR results is that at room temperature the quinone moieties are rotating through the calixarene cavity while the two aromatic rings remain fixed relative to one another. As the temperature is lowered, this dynamic process is slowed on the NMR time scale and the quinone groups adopt fixed cone and partial cone conformations. Figure 4 shows the ¹H NMR spectrum of **1** in dichloromethane-*d*₂ at 191 K. The methylene region of the NMR spectrum (between 2.8 and 5.4

(28) Beer, P. D.; Drew, M. G. B.; Gale, P. A.; Leeson, P. B.; Ogden, M. I. *J. Chem. Soc., Dalton Trans.* **1994**, 3479.

(29) Casnati, A.; Comelli, E.; Fabbri, M.; Bocchi, V.; Mori, G.; Ugozzoli, F.; Lanfredi, A. M. M.; Pochini, A.; Ungaro, R. *Recl. Trav. Chim. Pays-Bas* **1993**, 112, 384.

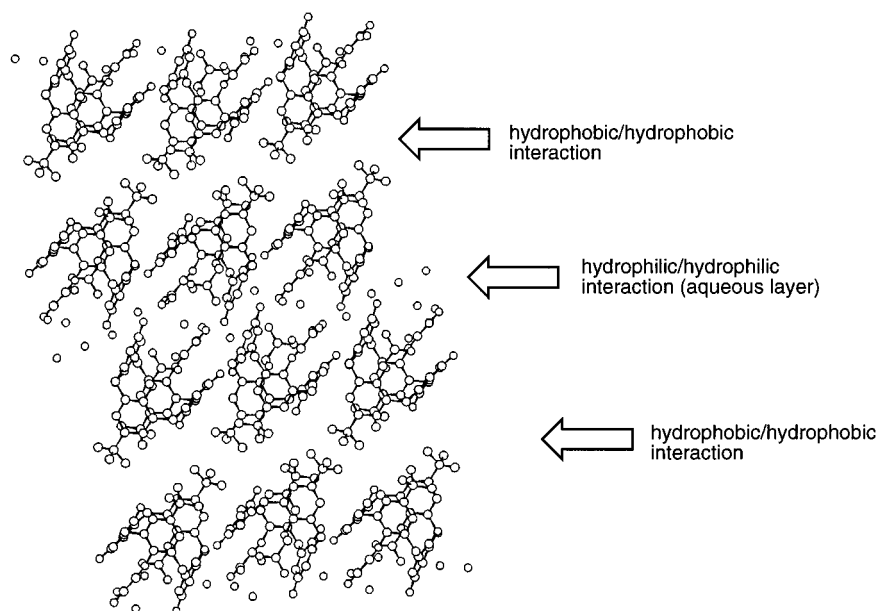
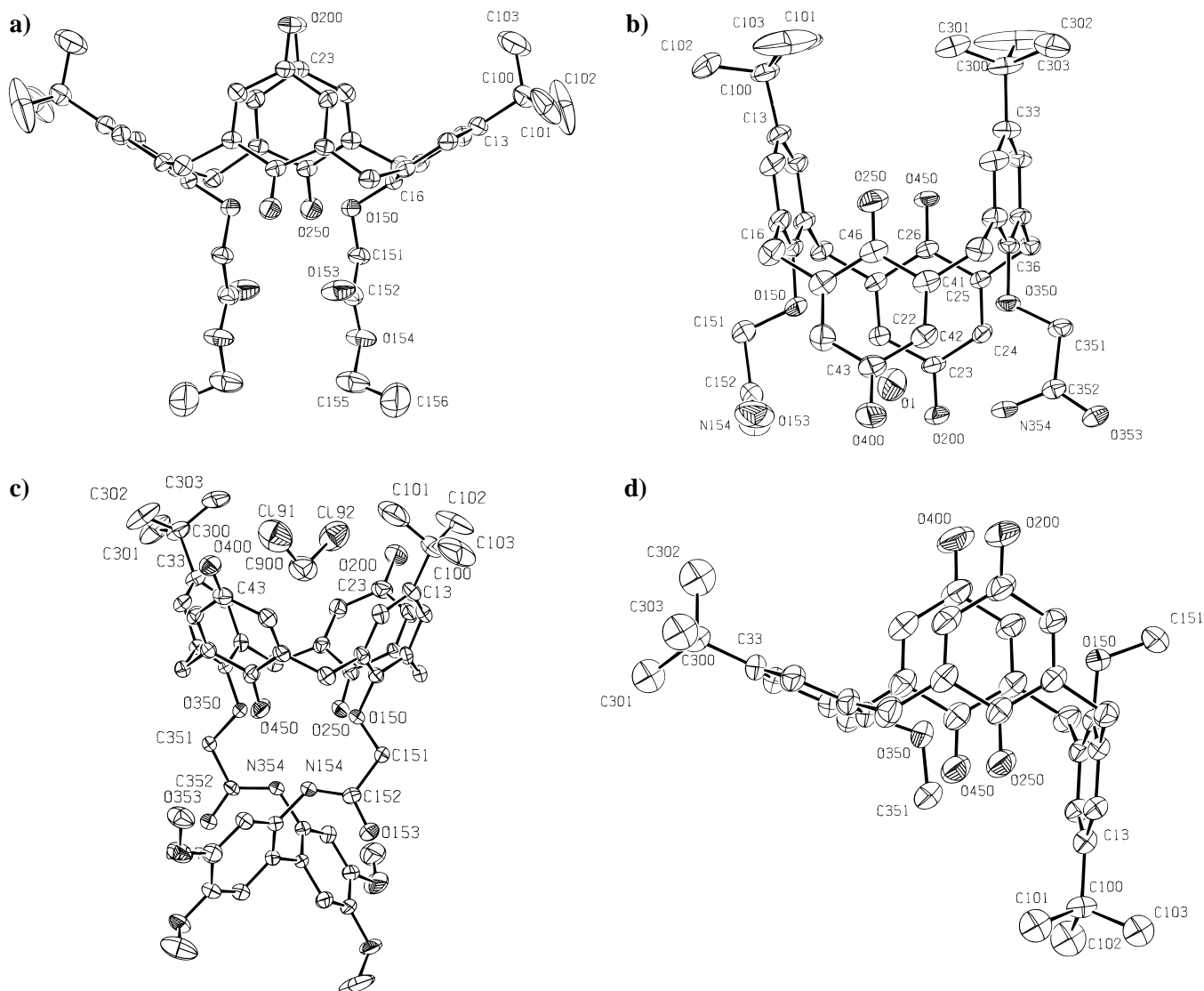


Figure 2. Packing diagram of $2 \cdot 3.5\text{H}_2\text{O}$ showing hydrophilic/hydrophilic layers.

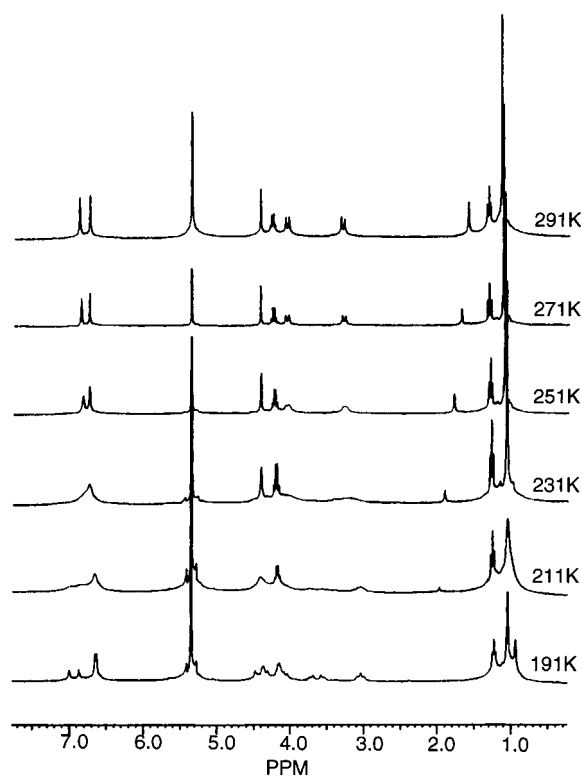
ppm) is not particularly sharp; however, the conformational behavior of this molecule can be determined from the splitting pattern. The cone isomer has only one type of ArCH_2Qu carbon

(λ) and hence will produce the usual AB splitting pattern. The partial cone isomer has two types of ArCH_2Qu carbons (μ and ν), and these will give two sets of AB patterns (four doublets).

Table 3. Dimensions of Hydrogen Bonds (Distances, Å) in the Structures^a

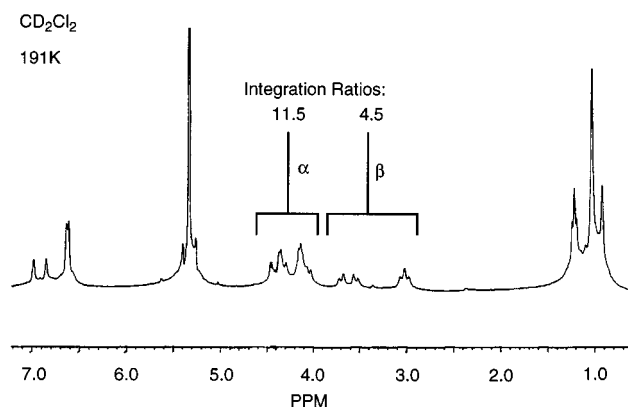
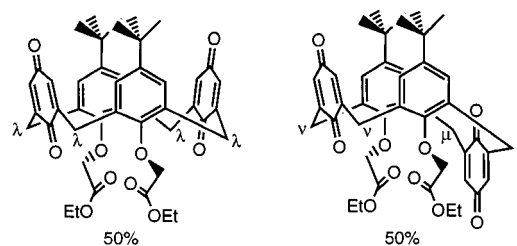
(a) 2·3.5H ₂ O			
O(1)···O(4)	2.825(7)	O(3)···O(353)	2.760(6)
O(1)···N(354)	2.908(6)	O(3)···O(153) ^{iv}	2.825(6)
O(1)···O(150)	3.018(5)	O(3)···O(2) ^v	2.905(8)
O(2)···O(200)	2.752(6)	O(3)···N(154) ^v	2.999(7)
O(2)···N(154) ⁱ	2.900(10)	O(3)···O(4) ^{iv}	3.093(10)
O(2)···O(3) ⁱⁱ	2.905(8)	O(200)···N(354) ⁱⁱⁱ	3.044(5)
O(2)···O(400) ⁱⁱⁱ	2.993(8)		
(b) 2·NaClO ₄			
O(13)···N(154) ^{vi}	3.12(1)	O(14)···N(154)	3.19(1)
O(13)···N(354) ^{vii}	3.12(1)		
(c) 4- <i>n</i> -BuNH ₃ BF ₄ ·0.25H ₂ O			
N(500)···O(250B)	2.847(13)	N(600)···O(353A)	2.868(18)
N(500)···O(450B)	2.827(12)	N(600)···O(450A)	2.848(14)
N(500)···O(353B)	2.931(13)	N(600)···O(250A)	2.845(13)
N(500)···O(153B)	2.942(13)	N(600)···O(153A)	2.974(12)
N(500)···O(200A)	3.048(13)	N(600)···O(400B)	2.947(15)
N(500)···O(350B)	3.073(12)	N(600)···O(150A)	3.087(12)
N(500)···O(150B)	3.055(12)	N(600)···O(350A)	3.137(12)
(d) 7			
N(154)···O(450)	2.840(11)	N(354)···O(250)	3.028(10)

^a Symmetry transformations used to generate equivalent atoms: (i) $-x, -y - 1, -z + 1$; (ii) $-x, y - 1, -z + 1/2$; (iii) $-x, y, -z + 1/2$; (iv) $x, 1 + y, z$; (v) $-x, 1 + y, -z + 1/2$; (vi) $-x, -y, 1 - z$; (vii) $-x, 2 - y, 1 - z$.

**Figure 3.** Variable-temperature ¹H NMR (300 MHz, dichloromethane-*d*₂) of compound **1** from 291 to 191 K.

This is observed in the β -region of the spectrum in Figure 4. The α -region includes the resonances from the λ -methylenes and the OCH₂ and COCH₂ resonances from both conformers. The relative integration of these regions is in the ratio 11.5/4.5 (α/β). Therefore, the ArCH₂Qu proton resonances from the cone and partial cone are in the ratio 3.5:4.5. At low temperatures, then, the methylene proton resonances suggest that, in dichloromethane-*d*₂ solution, **1** exists as approximately a 50:50 mixture of cone and partial cone conformers.

Coordination Studies in Solution. (a) ¹H NMR Titrations. NMR spectroscopy was used to investigate the solution complexation properties of **1–4**, **5**, **7**, and **8** with group 1 and 2

**Figure 4.** ¹H NMR spectrum of compound **1** at 191 K showing the presence of both cone and partial cone isomers in solution (top).

metal, ammonium, and alkylammonium cations. Unfortunately, due to the differing solubilities of calixdiquinone derivatives, a variety of solvents were employed.

In a typical titration experiment, the stepwise addition of a cation salt solution in 3/2 (v/v) chloroform-*d*/acetonitrile-*d*₃ to a solution of compound **1** (10 mM) in the same solvent mixture resulted in significant shifts of the receptor proton resonances (sodium perchlorate, potassium hexafluorophosphate, ammonium hexafluorophosphate, and *n*-butylammonium tetrafluoroborate) or the evolution of a new set of resonances (barium perchlorate) corresponding to a complexed species. The resulting titration curves (plotting δ (ppm) vs equivalents of cation added) indicate solution complexes of 1/1 stoichiometry with sodium, potassium, ammonium, and *n*-butylammonium cations. However, the titration curves were very sharp, and consequently, the stability constants were too high to be calculated using the EQNMR³⁰ least-squares nonlinear fitting procedure.

Interestingly, the difference in chemical shift between the AB pair of doublets of the methylene protons of compound **1** increases from 0.35 to 0.76 ppm on the addition of 1 equiv of barium cations. This observation may be attributed to the barium cation locking the calixarene into a cone conformation by complexing not only the ester carbonyl oxygen donor atoms but also interacting with the quinone carbonyl moieties. This mode of metal cation coordination would have the effect of inhibiting the quinone calix-ring inversion process and consequently rigidifying the receptor into a cone conformation. Indeed, in support of this hypothesis, a low-temperature ¹H NMR spectrum of **1** in the presence of barium cations exhibited exclusively one pair of doublets for the methylene protons.

Compound **4** exhibits complexation behavior similar to that of compound **1**. The addition of substoichiometric quantities of barium or sodium perchlorate to a solution of ligand in acetonitrile-*d*₃ caused a new set of resonances to evolve. In contrast, the addition of other salts (potassium hexafluorophosphate, ammonium hexafluorophosphate, and *n*-butylammonium tetrafluoroborate) resulted in shifts of the proton resonances indicative of 1/1 cation/calixdiquinone stoichiometry. The stability constants of these complexes were again too high to accurately gauge from EQNMR analysis.³⁰

(30) Hynes, M. J. *J. Chem. Soc., Dalton Trans.* **1993**, 311.

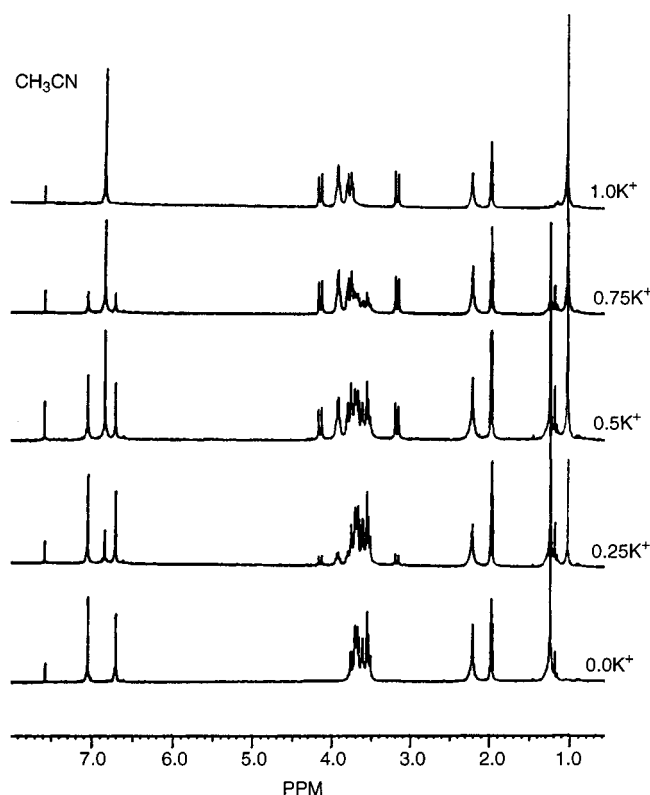


Figure 5. New resonances evolving in the ^1H NMR spectrum of compound **5** over the addition of 1.0 equiv of potassium cations.

Surprisingly, with solutions of compound **2** in chloroform-*d* the addition of these salts resulted in no significant shift of any of the receptor proton resonances. This behavior may be due to intramolecular $\text{NH}\cdots\text{O}=\text{C}$ hydrogen bonds, which inhibit the complexation process. Indeed, ^1H NMR titrations with the *n*-butyl secondary amide compound **3** in acetonitrile-*d*₃ showed only weak ammonium binding and no interaction with *n*-butylammonium cations (supporting the intramolecular amide $\text{NH}\cdots\text{O}=\text{C}$ interaction). In an attempt to disrupt the hydrogen-bonding network, a polar protic solvent, methanol-*d*₄, was employed. Titrations of **2** with potassium and ammonium hexafluorophosphate caused only very small shifts in the proton resonances; however, addition of sodium perchlorate caused an upfield shift of both the aromatic and methylene proton signals. The stability constant for the sodium complex was calculated using the EQNMR program³⁰ and found to be $3.5 \times 10^2 \text{ M}^{-1}$ ($\pm 5\%$) in methanol-*d*₄. The evolution of a new set of resonances corresponding to solution-complexed species were observed upon addition of barium cations. Unfortunately, due to solubility problems, a comparable set of titrations could not be performed with compound **3** in methanol-*d*₄.

Titration experiments were carried out with compound **5** in acetonitrile-*d*₃/chloroform-*d* (4/1, v/v) solution and showed the evolution of a new set of resonances with sodium, potassium, ammonium, *n*-butylammonium, and barium cations. Figure 5 shows the changes in the ^1H NMR spectrum of **5** upon addition of potassium cations. These new resonances evolved over the course of the addition of 1.0 equiv of cation, suggesting 1/1 solution complex stoichiometry in which the cationic guest is bound *via* favorable ion-dipole interactions with the crown polyether oxygen donor atoms and the quinone carbonyl moieties of **5**.

The introduction of barium cations to a chloroform-*d* solution of compound **7** had no effect on the ^1H NMR spectrum. This is perhaps unsurprising, as the biphenyl group is blocking the binding site, thus preventing the barium cation from interacting with the quinone carbonyl oxygens. Also, the amide NH groups

Table 4. Stability Constants ($\log K$)^a of **1–5** and **8** with Cations in Various Solvents at 296 K

salt	$\log K$						<i>e</i>
	1 ^b	2 ^c	3 ^d	4 ^d	5 ^d	5 ^c	
NaClO_4	>6.0	2.5	4.2	5.2	>6.0	5.0	<i>e</i>
KPF_6	4.8	2.1	3.5	4.7	>6.0	>6.0	4.3
$\text{Ba}(\text{ClO}_4)_2$	5.7	>6.0	5.2	5.3	>6.0	<i>f</i>	3.7
NH_4PF_6	4.0	3.5	2.0	3.1	>6.0	4.8	<i>g</i>
<i>n</i> -BuNH ₃ BF ₄	3.8	2.4	<i>g</i>	4.0	5.2	<i>f</i>	<i>g</i>

^a Maximum error estimated to be $\pm 10\%$. ^b Conducted in $\text{CH}_2\text{Cl}_2/\text{CH}_3\text{CN}$ (4/1, v/v). ^c Conducted in CH_3OH . ^d Conducted in CH_3CN . ^e Very small perturbation observed. ^f Binding profile would not fit 1/1 cation/ligand binding model. ^g No evidence of binding was observed.

are within hydrogen-bonding distance of the quinone oxygens and, hence, the lack of coordination may be due to a mixture of steric and/or intramolecular hydrogen-bonding interactions.

Ligand **8** displayed cation coordination behavior similar to that of **4**, except that no evidence of complexation of ammonium cations was observed.

(b) UV/Vis Spectroscopic Investigations. By monitoring the perturbation of the n to π^* electronic transition of the quinone moiety on addition of cationic guest, UV/vis titrations were carried out on the calixdiquinone receptors and stability constants calculated using the SPECFIT program.¹⁵

Table 4 shows that, in the case of compound **1**, barium forms a complex which is at least 1 order of magnitude more stable than those with potassium, ammonium, or *n*-butylammonium cations. This is not surprising, considering the charge difference between these guests. The stability constant with sodium cations was too high to be elucidated by UV/vis spectroscopic techniques. The high stability constant of the **1**-Na complex may be due to the optimal spatial fit of the sodium cation within the cavity of the calixdiquinone. In contrast, compound **8** shows no evidence of any interaction with ammonium or *n*-butylammonium cations. The stability constant values of the potassium or barium complexes of **8** are lower than those of the potassium or barium complexes of **1**, presumably due to the absence of the ester carbonyl groups in compound **8**.

The cation stability constant values of **2–4** are shown in Table 4. Again, due to solubility problems the titrations could not all be carried out in the same solvent. All three ligands exhibit a selectivity preference for the barium cation and form more thermodynamically stable complexes with sodium over potassium cations. It is noteworthy that **2**, even in methanol, forms a complex with the ammonium cation with a larger stability constant value than with either sodium or potassium. The low stability constant value of **3** with ammonium cations and also its failure to interact with *n*-butylammonium cations may be accounted for by intramolecular hydrogen bonding between the quinone or amide carbonyl and the amide NH group in acetonitrile solution.

The results of analogous experiments with **5** in acetonitrile and methanol solutions are also presented in Table 5. The magnitudes of the cation stability constants for **5** are much larger than for the lower rim acyclic ester, amide and methoxy calix-[4]diquinone analogues. In acetonitrile solution the stability constant values are so large that only an estimated lower limit value can be given. Even in methanol solution very stable complexes are formed with the selectivity trend $\text{K}^+ > \text{Na}^+ > \text{NH}_4^+$ being displayed. Surprisingly, the barium and *n*-butylammonium cation titration curves could not be fitted to a 1/1 cation/calixdiquinone binding model, and SPECFIT¹⁵ analysis suggested the presence of additional 2/1 (and other binding ratio) complex species in methanol solution, which precluded reliable stability constant values from being determined with these cationic guests.

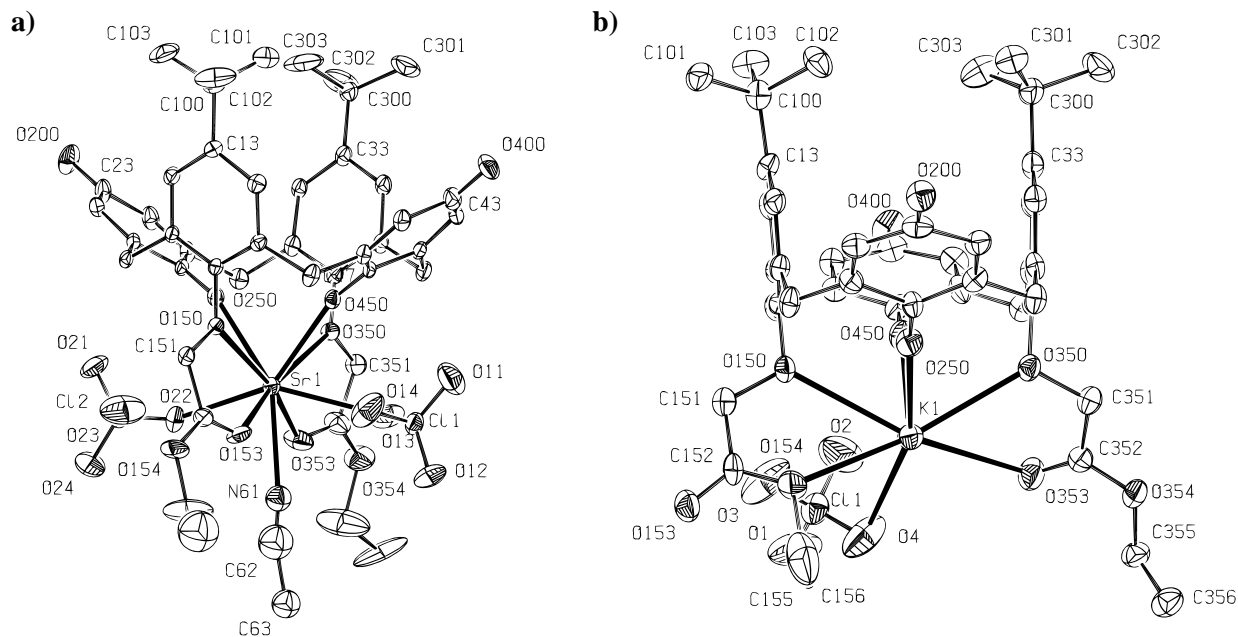


Figure 6. X-ray crystal structures of (a) **1**-Sr(ClO₄)₂·0.5NCMe and (b) **1**-KClO₄. Thermal ellipsoids are shown at the 5% probability level for (a) and the 25% probability level for (b).

Table 5. Bond Lengths (Å) in the Metal Coordination Spheres^a

(a) Strontium Coordination Sphere in 1 -Sr(ClO ₄) ₂			
Sr(1)–O(153)	2.566(10)	Sr(1)–O(22)	2.63(2)
Sr(1)–O(353)	2.574(11)	Sr(1)–O(150)	2.773(6)
Sr(1)–O(450)	2.596(8)	Sr(1)–O(13)	2.78(2)
Sr(1)–O(250)	2.628(8)	Sr(1)–O(350)	2.798(7)
Sr(1)–N(61)	2.61(3)		
(b) Potassium Coordination Sphere in 1 -KClO ₄			
K(1)–O(450)	2.603(7)	K(1)–O(4)	2.88(1)
K(1)–O(1)	2.635(9)	K(1)–O(154)	2.922(8)
K(1)–O(250)	2.695(8)	K(1)–O(150)	2.974(8)
K(1)–O(350)	2.836(9)	K(1)–O(353)	3.049(9)
(c) Sodium Coordination Sphere in 2 -Na(ClO ₄)·2MeOH			
Na(2)–O(250)	2.315(9)	Na(2)–O(400) ⁱ	2.410(7)
Na(2)–O(350)	2.537(6)	Na(2)–O(150)	2.376(7)
Na(2)–O(353)	2.315(7)	Na(2)–O(153)	2.380(9)
Na(2)–O(450)	2.306(6)		
(d) Sodium Coordination Sphere in 5 -Na(CF ₃ CO ₂)			
Na–O(150)	2.713(6)	Na–O(350)	2.709(5)
Na–O(153)	2.991(8)	Na–O(250)	2.522(6)
Na–O(156)	2.622(8)	Na–O(450)	2.302(7)
Na–O(159)	2.901(9)	Na–O(62)	2.249(9)
(e) Potassium Coordination Sphere in 5 -KClO ₄			
K(1)–O(450)	2.633(5)	K(1)–O(159)	2.874(6)
K(1)–O(250)	2.636(5)	K(1)–O(153)	2.930(6)
K(1)–O(156)	2.740(6)	K(1)–O(2)	2.945(10)
K(1)–O(150)	2.819(5)	K(1)–O(3)	2.976(12)
K(1)–O(350)	2.820(4)		

^a Symmetry transformations used to generate equivalent atoms: (i) $x - 1, y, z$.

Coordination Studies in the Solid State. Crystalline complexes of the calixdiquinone ligands were obtained by slow evaporation of a solution of the ligand in the presence of excess cation salt. Elemental analysis revealed that all the solid-state complexes obtained had 1/1 cation/ligand stoichiometry. Typically, the cation salt was dissolved in ethanol and added to a dichloromethane solution of the ligand. Slow evaporation of the solvent mixture afforded, in some cases, single crystals suitable for X-ray crystallographic analysis. Hydrogen bonding and metal coordination sphere distances are given in Tables 3 and 5, respectively. Crystals of the strontium complex of **1** were grown from a dichloromethane/ethanol mixture of ligand and Sr(ClO₄)₂. The strontium complex **1**-Sr(ClO₄)₂ (Figure 6a) adopts the flattened-cone conformation in the solid state

(aromatic rings 79.8(3), 81.4(3)°, quinone rings 37.4(3), 38.4(3)°). The strontium cation is nine-coordinate, being bound by six oxygens from the calix[4]diquinone, two oxygens from two perchlorates, and one nitrogen from a solvent acetonitrile. This acetonitrile had less than expected electron density, and refinement proved more successful with 50% occupancy than with high thermal parameters. Bond lengths are as expected for strontium with the shortest distances to the ester carbonyl oxygens Sr(1)–O(153) = 2.566(10), Sr(1)–O(353) = 2.574(11) Å, and quinone oxygens Sr–O(250) = 2.628(8), Sr–O(450) = 2.596(8) Å. Other bonds are to the acetonitrile (Sr–N(61) = 2.61(3) Å) and the perchlorates (Sr–O(22) = 2.63(2), Sr–O(13) = 2.78(2) Å), with the longest bonds to the ethereal oxygens at the lower rim of the cavity being 2.773(6) and 2.798(7) Å.

For **1**-KClO₄ (Figure 6b) the potassium ion is coordinated to one ester group *via* the carbonyl oxygen O(353) (3.049(9) Å); however, interestingly, the other ester group is flipped so that coordination to the potassium ion is *via* the acyl oxygen (K–O(154) = 2.922(8) Å). The quinone oxygen atoms O(250) and O(450) are also closely coordinated to the potassium ion (2.695(8) and 2.603(7) Å), while the ethereal oxygen atoms O(150) and O(350) are more distant (2.974(9) and 2.836(9) Å). The perchlorate counterion is also coordinated closely through two of its oxygen atoms to the potassium (K(1)–O(1) = 2.635(9), K(1)–O(4) = 2.88(1) Å).

In contrast with the structure of **2**·3.5H₂O, the sodium complex **2**-NaClO₄ adopts the cone conformation with the aromatic rings perpendicular and the quinone rings pseudohorizontal to the methylene plane (Figure 7). The sodium atom is seven-coordinate, being bonded to the six oxygen atoms at the lower rim and, in addition, to an upper rim quinone oxygen from an adjacent molecule. The bonds are to the lower rim quinones Na(2)–O(250) = 2.315(9), Na(2)–O(450) = 2.306(6) Å, to the amide carbonyls Na(2)–O(153) = 2.380(9), Na(2)–O(353) = 2.315(7), and to the ethereal oxygen atoms Na(2)–O(150) = 2.376(7) and Na(2)–O(350) = 2.537(6) Å. A further bond is formed to an upper rim quinone oxygen atom from an adjacent molecule at 2.410(7) Å. Thus, the complexes form a one-dimensional chain in the crystal, which is shown in Figure 7. The perchlorate anion does not bond to the sodium

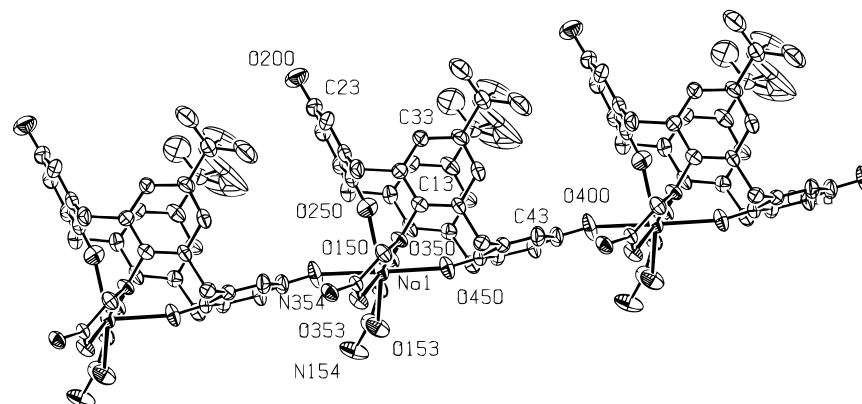


Figure 7. Structure of 2- $\text{Na}(\text{ClO}_4)$. The complex forms a one-dimensional coordination chain in the crystal. Thermal ellipsoids are shown at the 25% probability level.

cation but instead forms three hydrogen bonds to the two amide groups ($\text{O}-\text{N} = 3.18(1), 3.12(1), 3.11(1) \text{ \AA}$).

In 4-*n*- BuNH_3BF_4 , calix[4]diquinone **4** is complexed to an *n*-butylammonium cation. There are two such complexes in the asymmetric unit together with disordered BF_4^- anions. The conformations of both calix[4]diquinones are similar with vertical aromatic rings ($85.6(3), 88.9(3), 82.8(4), 89.0(3)^\circ$) and near-horizontal quinone rings ($23.9(2), 28.4(5), 36.8(5), 27.1(3)^\circ$). The dimer is shown in Figure 8, which portrays the *n*-butylammonium cation in the cavity at the lower rim. The nitrogen atoms of the two *n*-butylammonium ions bound to the lower rim of the calixdiquinones are in close contact with six oxygen atoms in the range $2.85(1)–3.14(1) \text{ \AA}$. In addition, there is a further close contact of one of the nitrogen atoms with the other calixdiquinone molecule *via* an upper rim quinone oxygen ($2.95(1), 3.05(1) \text{ \AA}$). This additional bond is a feature of diquinone structures that is in contrast with the case for the parent calix[4]arene structures; the ability of the quinone group to bond *via* the upper rim as well as the lower is also apparent in the sodium complex 2- $\text{Na}(\text{ClO}_4)$ and the ammonium complex 1- NH_4PF_6 .

Structures of 5- $\text{Na}(\text{OCOCF}_3)$ and 5- KClO_4 show a pseudo-15-crown-5 ring formed between the 1- and 3-oxygen atoms at the lower rim in which sodium and potassium ions are encapsulated (parts a and b of Figure 9). In both structures, the cone conformation is found with the aromatic rings near-perpendicular and the quinone rings near-horizontal (angles in Na structure $85.7(2), 78.9(2)^\circ; 32.3(2), 38.0(3)^\circ$ and in K structure $86.0(2), 79.4(2)^\circ; 31.4(2), 40.4(2)^\circ$). The sodium ion is eight-coordinate, being bonded to seven oxygen atoms at the bottom of the cone together with one oxygen atom from the CF_3CO_2^- counteranion. The shortest bonds are to the anion ($\text{Na}-\text{O}(62) = 2.249(9) \text{ \AA}$) and to the quinone oxygen atoms ($\text{Na}-\text{O}(250) = 2.522(6), \text{Na}-\text{O}(450) = 2.302(7) \text{ \AA}$). Other bonds are formed to the ethereal oxygen atoms O(150) at $2.713(6) \text{ \AA}$ and O(350) at $2.709(5) \text{ \AA}$ and to the crown oxygen atoms O(153) at $2.991(8) \text{ \AA}$, O(156) at $2.622(8) \text{ \AA}$, and O(159) at $2.901(9) \text{ \AA}$. These distances are unusually long for sodium (e.g. in 2- NaClO_4 the seven Na-O distances range from 2.30 to 2.55 \AA) and are indicative of the fact that the ring is too large for this ion. The five oxygen atoms in the ring are coplanar (maximum deviation 0.040 \AA), with the sodium cation 0.33 \AA from this plane.

In contrast, the K-O bond lengths in the structure are of the expected length. The potassium cation is bonded to nine oxygen atoms; the shortest bonds are to the lower rim quinone oxygen atoms ($\text{K}(1)-\text{O}(450) = 2.633(5)$ and $\text{K}(1)-\text{O}(250) = 2.636(5) \text{ \AA}$) and then the oxygen atoms in the crown ether bridge ($\text{K}(1)-\text{O}(156) = 2.740(6), \text{K}(1)-\text{O}(150) = 2.819(5), \text{K}(1)-$

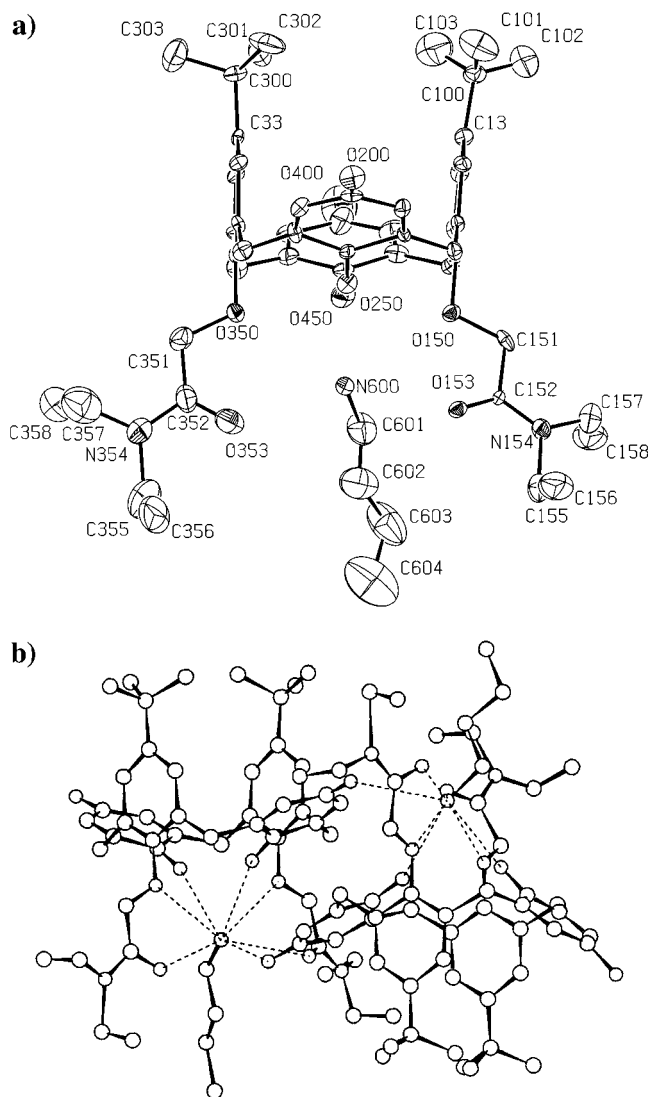


Figure 8. Structure of 4-*n*- BuNH_3BF_4 (a), which forms dimeric units in the crystal (b). Thermal ellipsoids are shown at the 15% probability level.

$\text{O}(350) = 2.820(4), \text{K}(1)-\text{O}(159) = 2.874(6),$ and $\text{K}(1)-\text{O}(153) = 2.930(6) \text{ \AA}$). The cation is also chelated by a perchlorate ($2.976(12), 2.945(10) \text{ \AA}$). It is noteworthy that, in comparison with the cation complexes of the acyclic derivatives, these two structures show no intermolecular interactions with quinone oxygen atoms from other calix[4]diquinones. In this structure the five oxygen atoms in the crown are planar to within 0.10 \AA , with the potassium cation 0.43 \AA from the plane. The potassium cation is clearly too large for the crown.

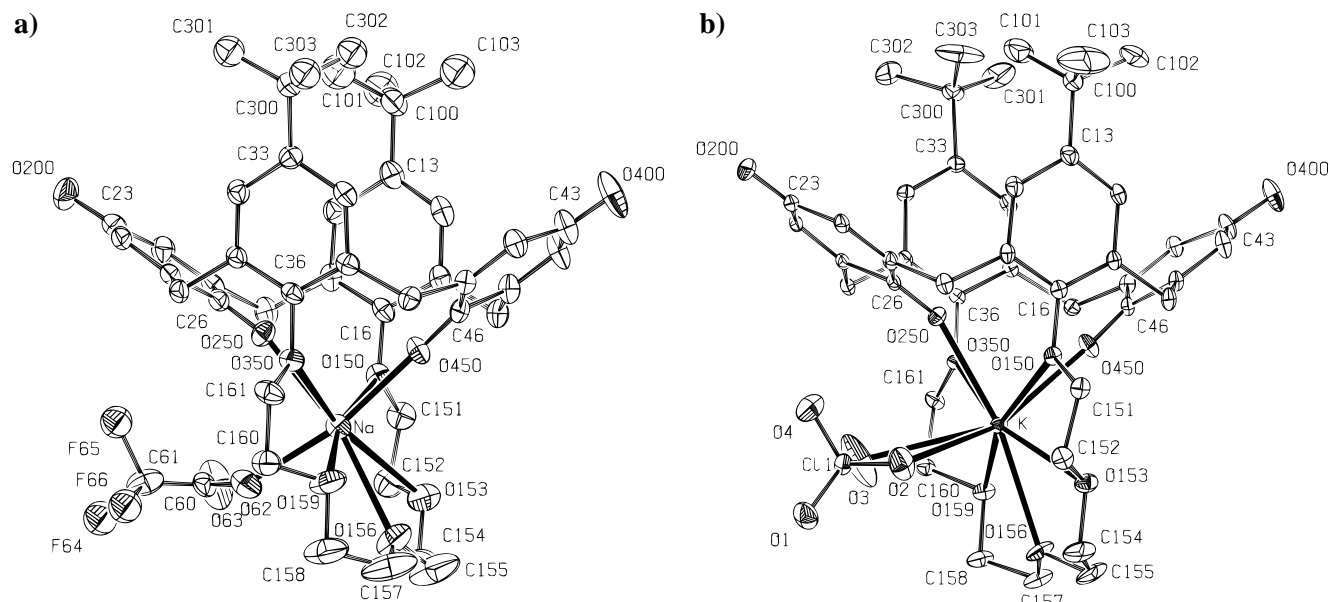


Figure 9. Structure of (a) 5-Na(CF₃CO₂) and (b) 5-KClO₄. Thermal ellipsoids are shown at the 5% probability level.

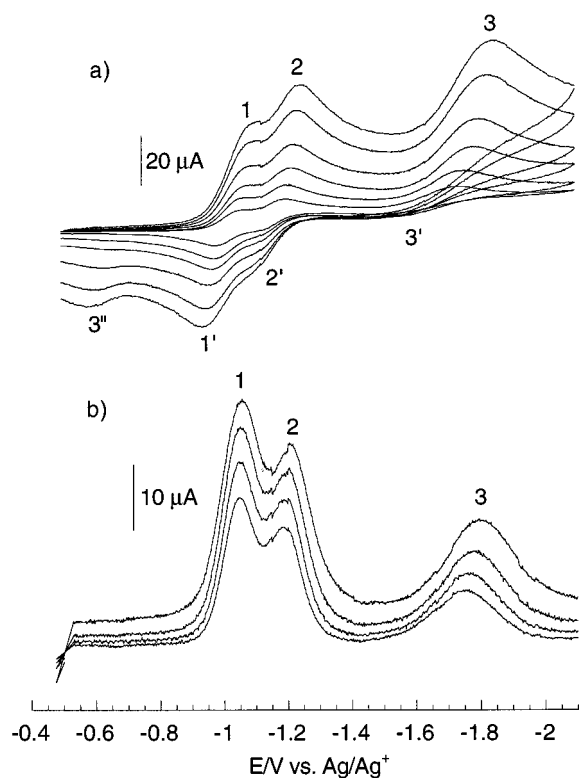


Figure 10. CVs (top) and SWVs (bottom) of **8** (1.4×10^{-3} M) recorded in CH₂Cl₂ at different scan rates and frequencies (in order of decreasing amplitude of current: CVs 600, 400, 200, 100, 50, 20 mV s⁻¹; SWVs 80, 40, 20, and 10 Hz).

Electrochemical Properties of Compounds **1**, **4**, and **8**.

The electrochemistry of ligands **1**, **4**, and **8** was investigated using cyclic and square wave³¹ voltammetric techniques.

A calixdiquinone can, in theory, accept a total of four electrons to become a tetraanion. Figure 10 shows cyclic voltammograms (CVs) of compound **8** in dichloromethane at different scan rates. For the convenience of discussion, each of the reduction waves is labeled with a number and each of the reoxidation waves with a number plus a prime (') or double prime (''). Compounds **1** and **4** exhibit CVs similar to those of

Table 6. CV Data Obtained from a 1:1 (v/v) Mixture of CH₃CN and CH₂Cl₂ at Room Temperature^a

compd	cathodic wave potential/mV				
	<i>E</i> _{c1}	<i>E</i> _{c2}	<i>E</i> _{c3} ^b	<i>E</i> _{c4}	<i>E</i> _{c5}
1	-1040	-1175	-1785	-820	
4	-1065	-1260	-1870	-740	-870
8	-1055	-1180	-1800		
compd	wave potential separation/mV				
	Δ <i>E</i> _{ac1}	Δ <i>E</i> _{ac2}	Δ <i>E</i> _{ac4}	Δ <i>E</i> _{ac5}	
1	85	100 ^c	90 ^d		
4	90	130 ^c	75	80	
8	85	90 ^c			

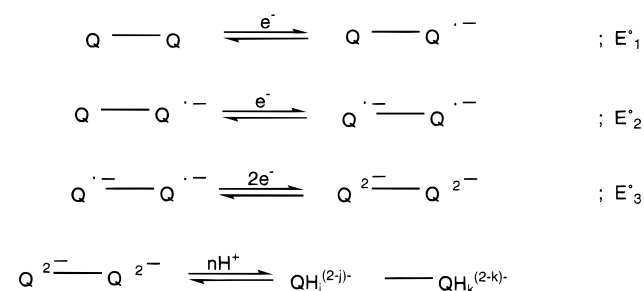
^a Maximum error is ±10 mV. Δ*E*_{ac*i*} (*i* = 1, 2, 4, 5) is the potential separation between the cathodic and anodic wave potentials. ^b Wave 3 is irreversible. ^c Estimated values. All CVs showed a poor resolution of wave 2'. ^d **1** showed only a broad prewave couple.

compound **8** under the same conditions, except that **1** and **4** show prewave couples (Table 6).

Wave couples 1/1' and 2/2' have previously been attributed to a one-electron transfer to each of the quinone moieties present in the molecule. The third and fourth electron transfers are believed to form wave 3. Casnati and co-workers suggested that the irreversibility of this wave could be due to the formation of CH₂Cl₂-insoluble hydroquinone species. This was supported by results from an exhaustive electrolysis of a calix[4]diquinone solution, which became nonelectroactive after the experiment. The one-wave feature of wave 3 may be due to a minimized repulsive interaction between the reduced quinone groups upon protonation, leading to a smaller potential separation between consecutive electron-transfer processes. This agrees with the observation that waves 1 and 2 merge into a single wave of typical EC shape after adding ammonium or *n*-butylammonium cations which may donate protons to the reduced quinone groups.

Considering the possible kinetics involved in wave 3 (a two-electron and four-proton transfer process), the aprotic nature of dichloromethane, and the potential of wave 3'', incompletely protonated quinone dianion species may be responsible for wave 3''. If this is the case, the observed increase in wave 3'' at fast scan rates can be easily explained by an EC mechanism. Its disappearance in the presence of acids or proton donors or in a less aprotic solvent such as acetonitrile or a mixture of

(31) Osteryoung, J.; O'Dea, J. J. In *Electroanalytical Chemistry*; Bard, A. J., Ed.; Dekker: New York, 1987; Vol. 14, p 209.

Scheme 1^a

^a Q, Q^{•-}, Q²⁻, QH_j^{(2-j)-}, and QH_k^{(2-k)-} ($n = j + k$; $j = 0, 1, 2$; $k = 0, 1, 2$; k and j may be different or equal) represent the neutral, radical anion, dianion, and the protonated dianion forms of the quinone moiety in the molecule; E_i° ($i = 1, 2, 3$) is the formal redox potential of the corresponding electron transfer reaction.

acetonitrile and dichloromethane may be due to faster and more complete protonation processes.

Combining the above discussions, the reduction of calix[4]-diquinones may be thought of as an EEEC mechanism (Scheme 1).

The quinone moieties in these molecules constitute not only the coordination site but also the redox-active center. The complexation processes can therefore be followed by electrochemical means. Owing to the poor solubility of metal salts in dichloromethane and compounds **1** and **8** in acetonitrile, the experiments were conducted in mixtures of these solvents (or in acetonitrile alone for **4**). The addition of 1 equiv or more of sodium perchlorate or potassium hexafluorophosphate to electrochemical solutions of **4** resulted in the disappearance of waves 1 and 2 and the evolution of reversible new wave couples at more anodic potentials. Figure 11 shows the cyclic voltammograms of **1** and **4** upon addition of sodium cations. Anodic potential perturbations were generally observed with **1**, **4**, and **8** and all cationic guests, and the results are summarized in Table 7.

Interestingly, addition of 1 equiv or more of ammonium hexafluorophosphate or *n*-butylammonium tetrafluoroborate to electrochemical solutions of **4** resulted in EC mechanistic behavior which was not affected by subsequent addition of equivalent amounts of Na⁺ or K⁺ cations. This finding is contrary to the respective stability constant data calculated from UV/vis titration results, in which the ammonium stability constant values are comparatively smaller in magnitude than those of the alkali-metal cations. The relatively strong interactions of these ammonium cations with the radical anions formed by the reduction of the respective quinone moieties of **4** may be responsible for this electrochemical observation and EC mechanistic behavior. In the presence of more than 1 equiv of barium perchlorate, both the cyclic and square wave voltammograms of **4** showed typical adsorption characteristics.

Electrochemical Properties of Compound 5. The electrochemistry and electrochemical cationic recognition studies of **5** were investigated using CV and SWV techniques, and the results are summarized in Table 8. The receptor itself undergoes a reversible reduction at -1.15 V and an irreversible redox process at -1.93 V (referenced to Ag/Ag⁺). Large anodic perturbations of the reduction waves were observed on addition of all the cationic guests, with Ba²⁺, which possesses the largest charge-to-radius ratio, producing the greatest effect ($\Delta E = 555$ mV). On addition of substoichiometric equivalents of Na⁺ cations the evolution of a new, substantially anodically shifted ($\Delta E = 255$ mV) redox couple results. After 1 equiv of Na⁺ has been added to the electrochemical solution, the uncomplexed original wave has disappeared (Figure 12). Thus, this novel *p*-*tert*-butylcalix[4]diquinone-crown-5 receptor not only forms thermodynamically very stable complexes with group 1 and 2

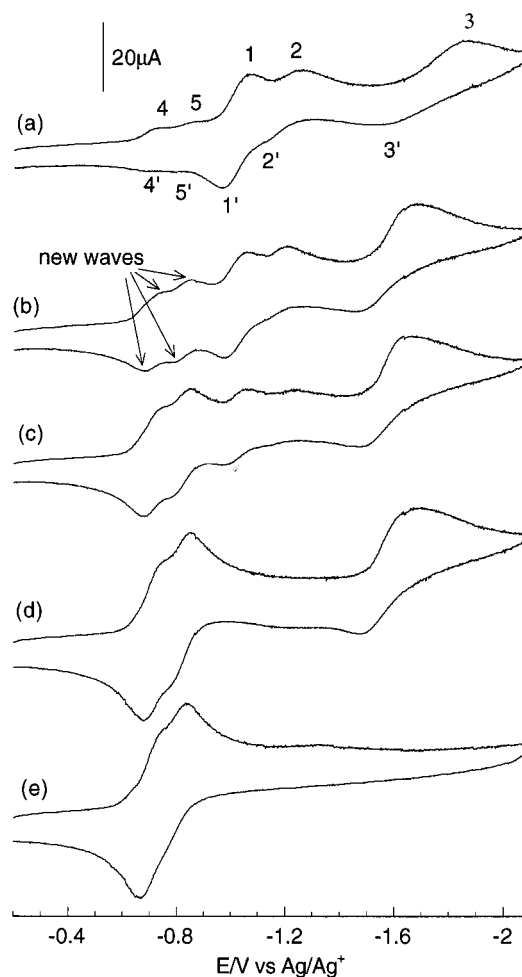


Figure 11. CVs of **4** (1.17×10^{-3} M) in a 1/1 mixture of CH₃CN and CH₂Cl₂ in the presence of different concentrations (equiv) of sodium cations: (a) 0; (b) 0.21; (c) 0.42; (d) 0.63; (e) 2.7. Scan rate: 100 mV s⁻¹.

Table 7. Summary of the Changes in Voltammetric Properties of **1** and **8** in 10% CH₂Cl₂/90% Acetonitrile and **4** in Acetonitrile upon Addition of 2.0 equiv of the Respective Cation^a

	E_{pc} (V) of each redox couple
Free 1	(-0.75 (s); -0.85 (r)); -1.10 (r); -1.24 (s)
+Na ⁺	-0.70 (r); -0.80 (s)
+K ⁺	-0.75 (s); -0.85 (r); -0.93 (r)
+Ba ²⁺	-0.52 (ec, a)
+NH ₄ ⁺	-0.67 (ec)
+ <i>n</i> -BuNH ₃ ⁺	-0.68 (ec)
Free 4	(-0.81 (r); -0.91 (r)); -1.11 (r); -1.26 (q))
+Na ⁺	-0.81 (r); -0.89 (r)
+K ⁺	-0.83 (r); -0.92 (r)
+Ba ²⁺	-0.64 (ec, a)
+NH ₄ ⁺	-0.69 (ec)
+ <i>n</i> -BuNH ₃ ⁺	-0.78 (ec)
Free 8	-1.05 (r); -1.09 (r)
+Na ⁺	-0.90 (r); -0.99 (s)
+K ⁺	-1.02 (r); -1.09 (r)
+Ba ²⁺	-0.52 (ec, a)
+NH ₄ ⁺	-0.85 (ec)
+ <i>n</i> -BuNH ₃ ⁺	-0.94 (ec)

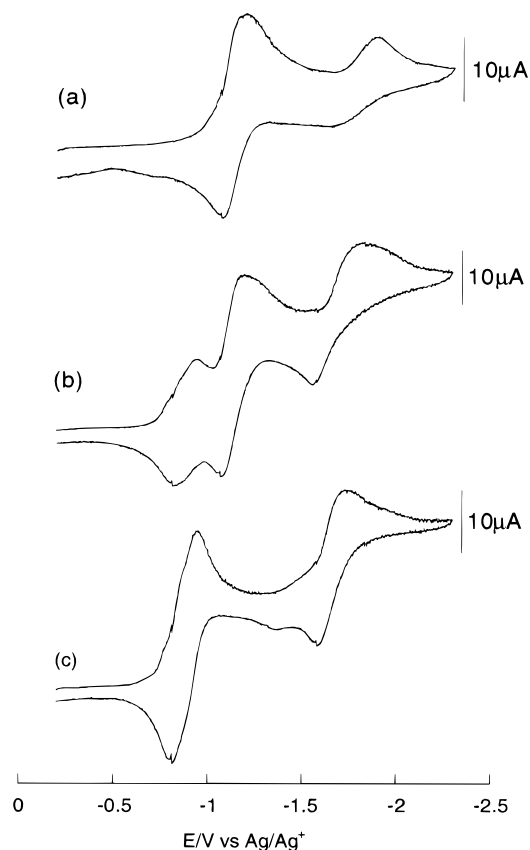
^a Supporting electrolyte 0.10 M *n*-Bu₄NBF₄. Definitions: E_{pc} , the potential of the a reduction current peak; r, reversible; q, quasi-reversible; s, single reduction peak without corresponding reoxidation peak; ec, electron transfer followed by a chemical reaction; ec, a, electron transfer followed by a chemical reaction with insoluble product which adsorbs onto the electrode surface. Prewaves are given in parentheses.

metal and ammonium cations but can also electrochemically sense these cationic species via substantial anodic perturbation effects.

Table 8. Reduction Potentials of **5** and the Anodic Shifts in the Presence of 1.0 or 2.0 equiv of Different Cationic Species^a

	E_{pc} (V) of each redox couple (vs Ag/Ag ⁺)	
	1.0 equiv	2.0 equiv
$E_{1/2}$ (free, V)	-1.155	-1.930
$\Delta E(K^+, mV)^b$	210	250
$\Delta E(Na^+, mV)^b$	255	290
$\Delta E(Ba^{2+}, mV)^b$	555	<i>d</i>
$\Delta E(NH_4^+, mV)^c$	405	<i>d</i>
$\Delta E(n-BuNH_3^+, mV)^c$	355	<i>d</i>

^a Obtained by both cyclic (100 mV s⁻¹) and square wave (10 Hz, Osteryoung-type) voltammetry in acetonitrile solution containing 0.1 M *n*-Bu₄NBF₄ as supporting electrolyte. Solutions were ca. 1 × 10⁻³ M in compound with reference to a Ag/Ag⁺ electrode (330 ± 10 mV vs SCE) at 21 ± 1 °C. ^b Anodic shift of the reduction waves of **5** in the presence of 1.0 equiv of the respective cationic species added as their perchlorate or hexafluorophosphate salts. ^c Anodic shift in the presence of 2.0 equiv of the respective cations. ^d The second reduction wave of **5** became obscure or disappeared in the presence of more than 1 equiv of the respective cations.

**Figure 12.** Cyclic voltammograms of **5** (1.0 × 10⁻³ M) in acetonitrile in the absence (a) and the presence of 0.3 equiv (b) and 1.0 equiv (c) of sodium cations added as the perchlorate salt. Scan rate: 100 mV s⁻¹.

Conclusions. A new series of ionophoric *p*-*tert*-butylcalix[4]diquinones containing ester (**1**), amide (**2–4**), crown ether (**5**), or a bis(veratrole) bridge (**7**) have been synthesized. The structures of the free ligands **1**, **2**, and **7** and the previously synthesized *p*-*tert*-butylcalix[4]diquinone bis(methyl ether) **8** have been elucidated by X-ray crystallography and found to adopt cone, 1,3-alternate, cone, and aryl partial cone conformations, respectively.

The coordination chemistry of these ligands has been studied with group 1 and 2 metal, ammonium, and alkylammonium cations by NMR and UV/vis spectroscopic techniques. Stability constant evaluations reveal that **1–4** generally form thermodynamically stable complexes with sodium, potassium, barium, ammonium, and *n*-butylammonium cations with the highest stability constant values being found with barium. The *p*-*tert*-butylcalix[4]diquinone–crown-5 ligand **5** forms much stronger complexes with these cations and in methanol solution exhibits the selectivity trend K⁺ > Na⁺ > NH₄⁺ with a log *K* value of >6.0 for K⁺.

The X-ray crystal structures of **1**-Sr(ClO₄)₂, **1**-KClO₄, **2**-NaClO₄, **4**-*n*-BuNH₃BF₄, **5**-NaCO₂CF₃, and **5**-KPF₆ have been elucidated, and it has been found that these complexes are exclusively in the cone conformation in the solid state. Cation–quinone oxygen atom coordination occurs at both the upper and lower rim of the calix[4]diquinone complexes **2**-NaClO₄ and **4**-*n*-BuNH₃BF₄, giving rise to one-dimensional chains of complexes and dimer formation, respectively. Intramolecular hydrogen bonding has been shown to play a role in the magnitude of the stability constants of compounds **2** and **3**. By blocking the lower rim binding site with a conformationally rigid bridging group (compound **7**), cation binding is suppressed.

The electrochemical properties of the lower rim acyclic ester, amide and methoxy derivatized *p*-*tert*-butylcalixdiquinones **1**, **4**, and **8** have been studied in various dichloromethane/acetonitrile solvent mixtures, and it has been found that in general these species undergo three distinct electron transfer processes (two one-electron transfers and a two-electron transfer). The potentials of the reductions are significantly anodically shifted in the presence of group 1 and 2 metal, ammonium, and alkylammonium guest cations, thus enabling these species to be used as prototype cation amperometric sensing devices. To the best of our knowledge this is the first time that the *n*-butylammonium cation has been detected by a redox-active ionophore. The potentials of these reduction processes of compound **5** are substantially shifted anodically in the presence of guest cations (by 555 mV in the presence of Ba²⁺) in a similar manner to that for **1**, **4**, and **8**.

The inclusion of this type of redox-active ionophore into membranes and electrochemically conducting polymeric supports may well produce novel molecular sensory devices of the future.

Acknowledgment. We thank the EPSRC for a quota studentship to P.A.G. and for use of the mass spectrometry service at the University of Wales, Swansea, Wales. We also thank the EPSRC together with the University of Reading for funds for the image plate system. The assistance of Mr. Simon W. Dent with the preparation of this paper is gratefully acknowledged.

Supporting Information Available: Text giving details of the X-ray experiments, tables of atomic positional parameters, bond lengths and angles, and atomic thermal parameters for the 10 structures presented in this paper, and figures giving additional NMR and UV/vis data for compounds **1–5** and **7** (113 pages). Ordering information is given on any current masthead page.